Positrons, electrons and γ-ray halos around pulsars

Fiorenza Donato
Torino University & INFN $ CERN

CDHY seminar, 04/06/2025

Galactic Cosmic Rays (CRs)

are charged particles (nuclei, isotopes, leptons, antiparticles)
diffusing in the Galactic magnetic field
Observed at Earth with E~ 10 MeV/n - 10^3 TeV/n

C. Evoli at https://agenda.infn.it/event/21891/

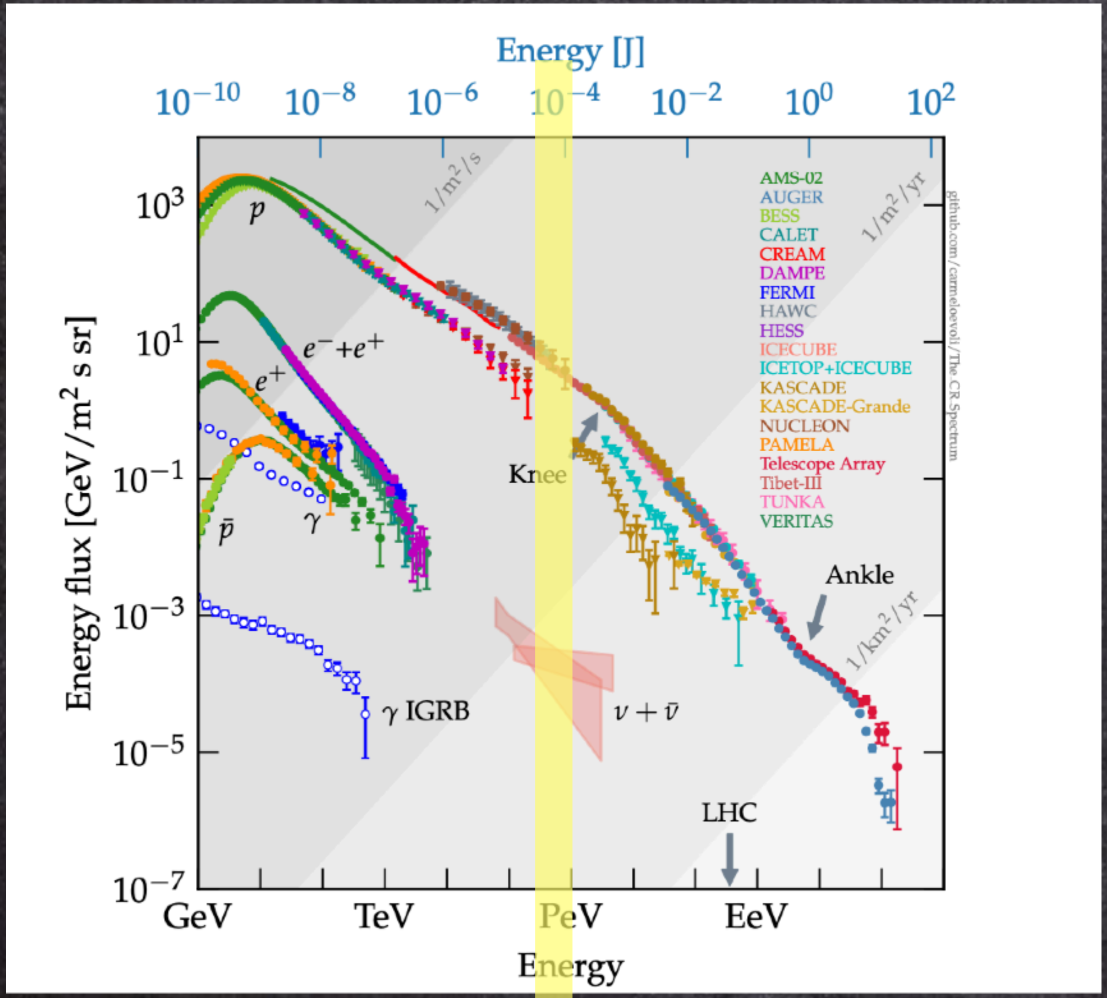

Direct measures

Air showers

Gabici, Evoli, Gaggero, Lipari, Mertsch, Orlando, Strong, Vittino 1903.11584

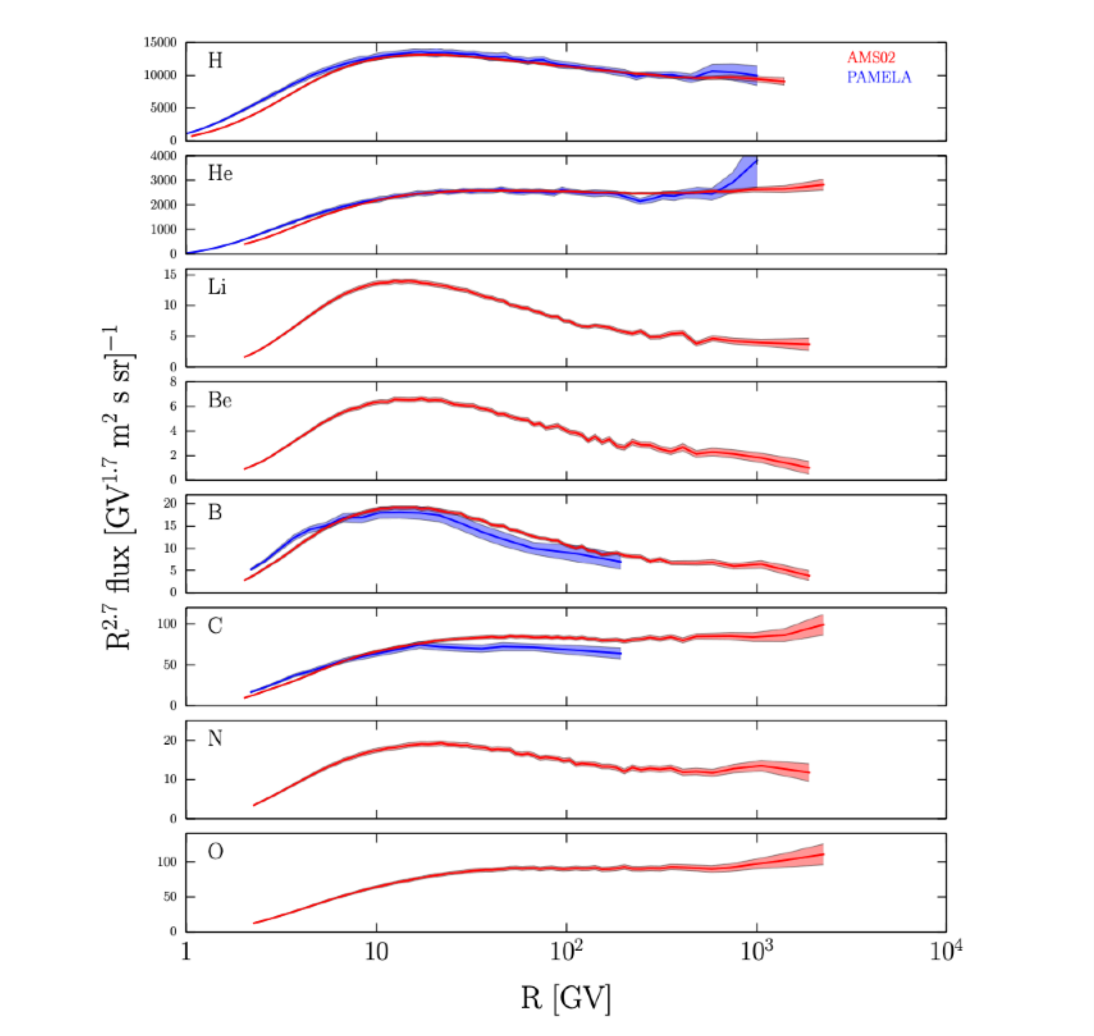

Fig. 1. The individual CR flux for nuclear species up to Oxygen as measured by PAMELA and AMS02. Shadow regions correspond to 1 sigma total errors (systematic and statistical added in quadrature).

CR database: D. Maurin+ EPJC 2023

See also N. Tomassetti 2301.10255

The observed electron spectrum

AMS Coll Phys.Rept. 2021

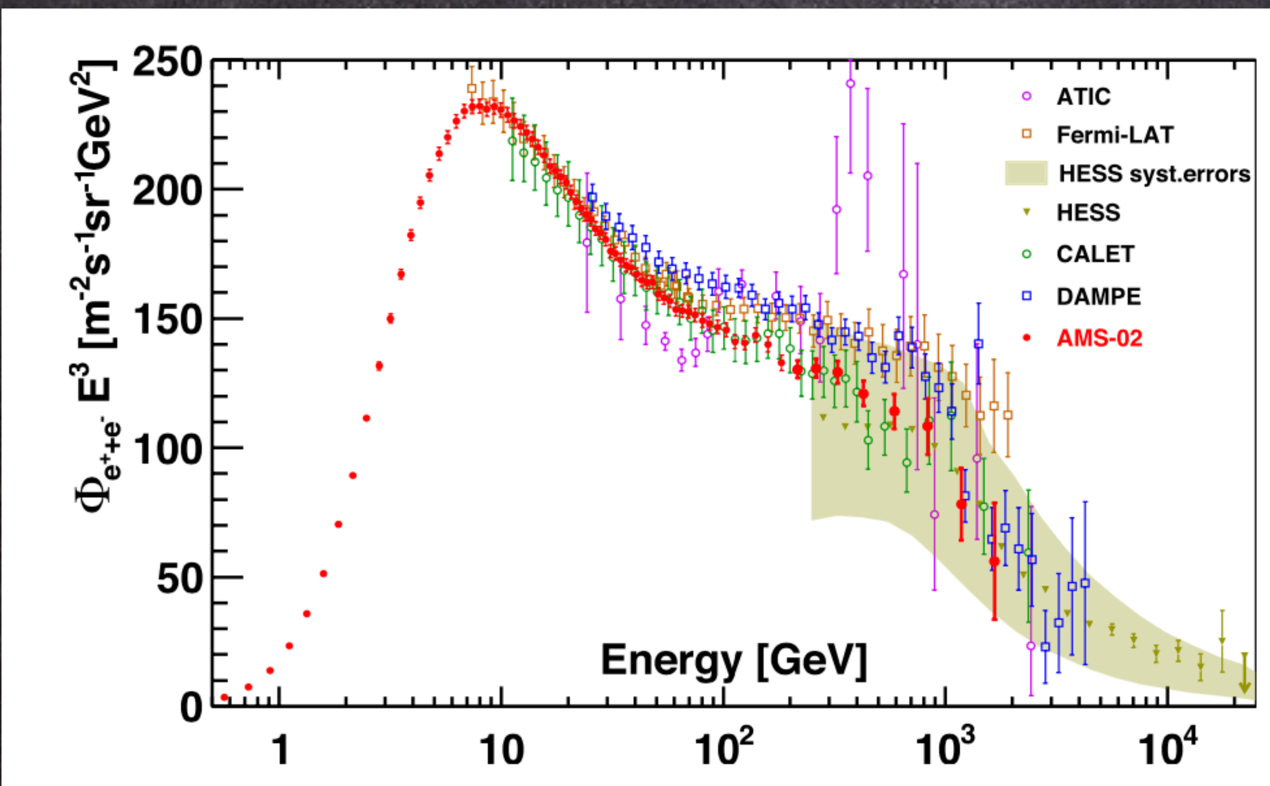

CALET Coll. PRL 2023

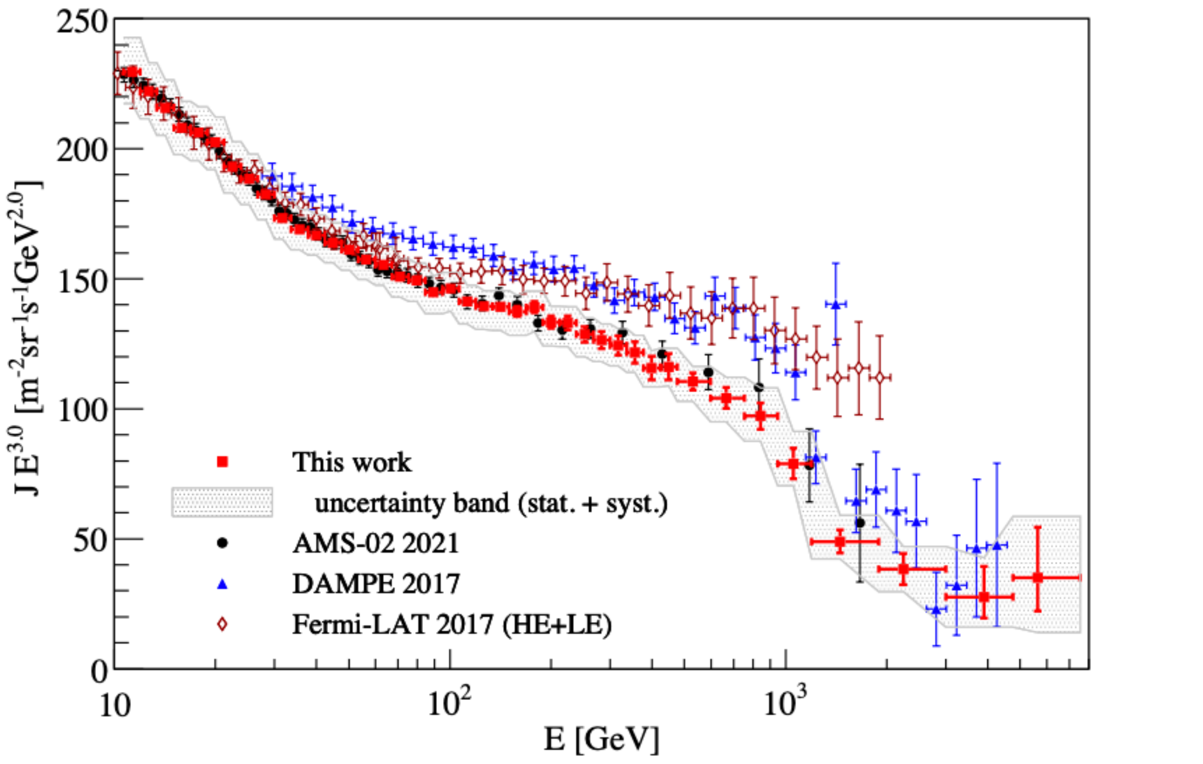

Data on total electron not fully compatible among them
A prominent break is observed at ~ TeV
still too uncertain to fix models. Pulsars can do the job

Propagation equation (tuned for leptons)

$$\frac{\partial \psi}{\partial t} - \nabla \cdot \{D(E)\nabla\psi\} + \frac{\partial}{\partial E}\left\{\frac{dE}{dt}\psi\right\} = Q(E, \mathbf{x}, t)$$

diffusion en. losses source spectrum

Diffusion: D(x,R) a priori
usually assumed isotropic in the Galaxy: $D \sim D_0 R^{\delta}$
D_0 and δ usually fixed by B/C

Energy losses: Nuclei: ionisation, Coulomb
Leptons: Synchrotron on the galactic B~3.6 μG
Inverse Compton on photon fields (stellar, CMB, UV, IR)

Sources: Supernova Remnants, $Q(E) \propto E^{-\gamma}$

Nuclear fragmentation, $Q_j(E) \propto n_{ISM}\, \sigma_{ij}\, \psi_i$

[Dark Matter annihilation or decay]

Detected e+ and e- are local

$$\lambda^2(E, E_S) = 4 \int_E^{E_S} dE' \frac{D(E')}{b_{\rm loss}(E')}$$

Typical propagation length in the Galaxy

Manconi, Di Mauro, FD JCAP 2017

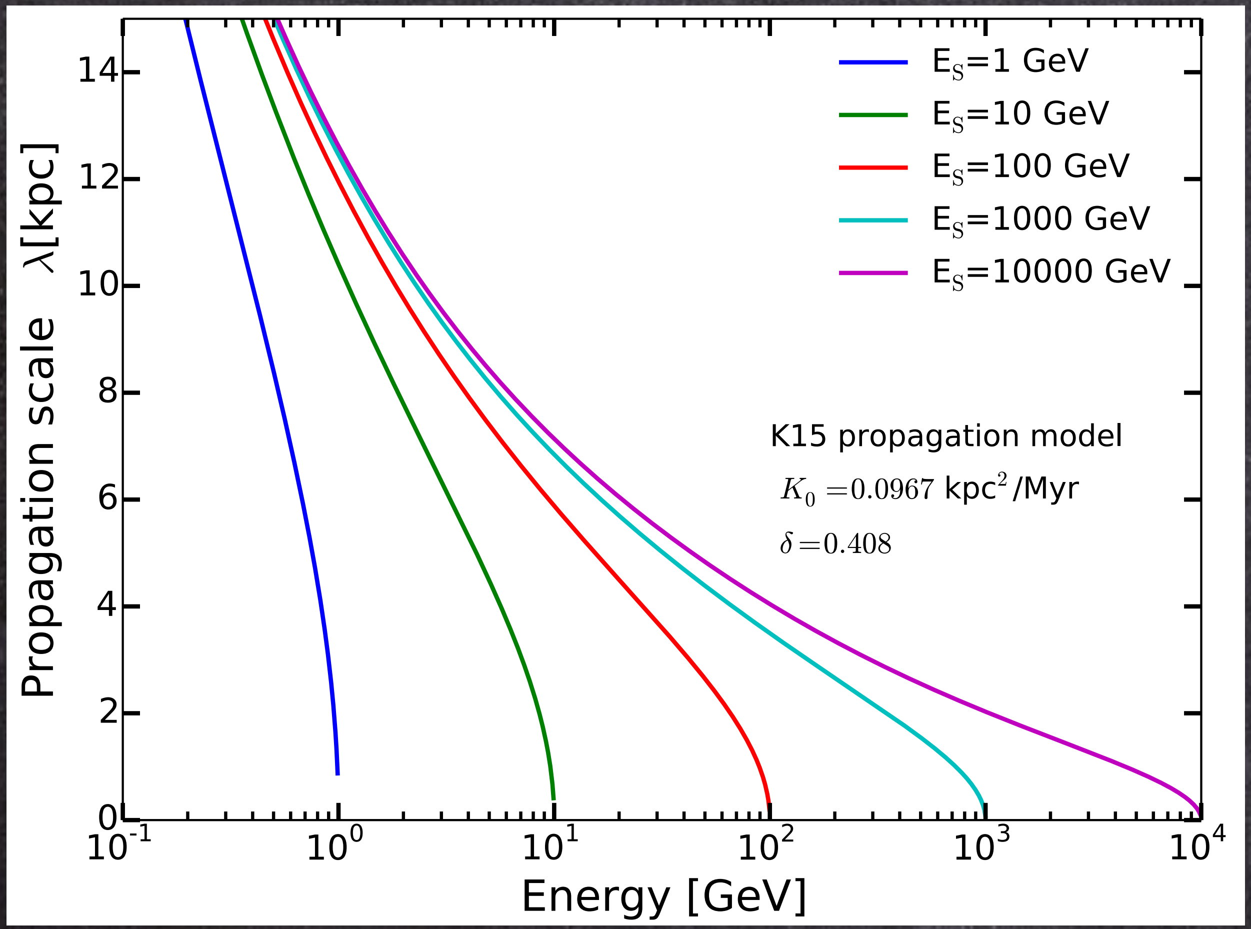

Sources of e+ & e- in the Galaxy

- Inelastic hadronic collisions (asymm.)
- Pulsar wind nebulae (PWN) (symm.)
- Supernova remnants (SNR) (only e-)
- Particle Dark Matter annihilation (e+,e-)?

e-, e+ suffer strong radiative cooling and arrive at Earth if produced within few kpc around it.

Local sources very likely leave their imprints in the spectra

Where is the end of the cosmic ray (CR) spectrum?

Sudoh & Beacom, PRD 2024

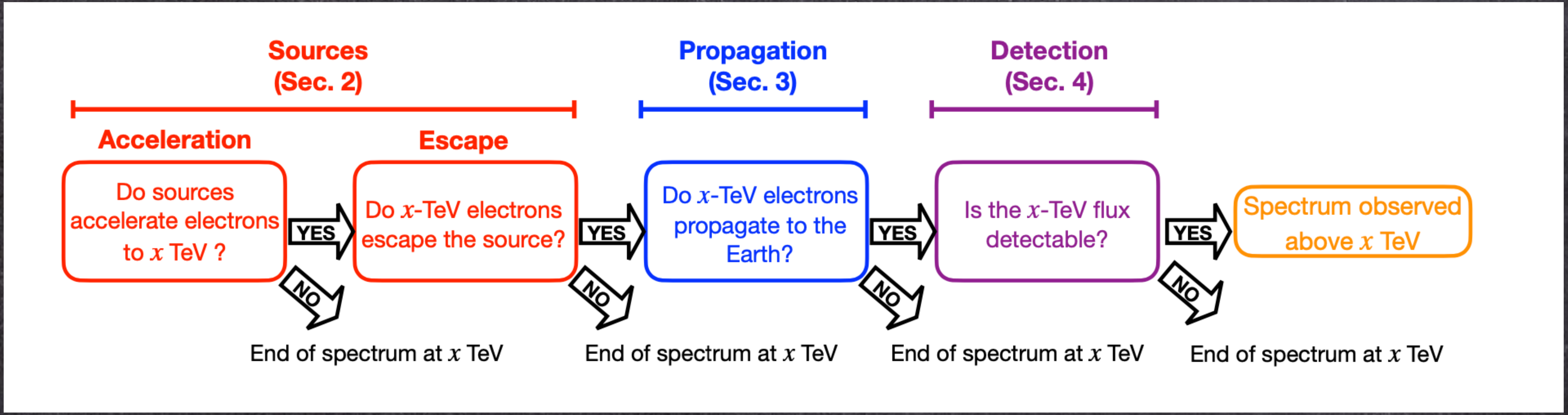

Robust electron detection up to few TeV

γ rays from pulsars are instead measured up to PeV energies

Cosmic ray experiments: species and energies

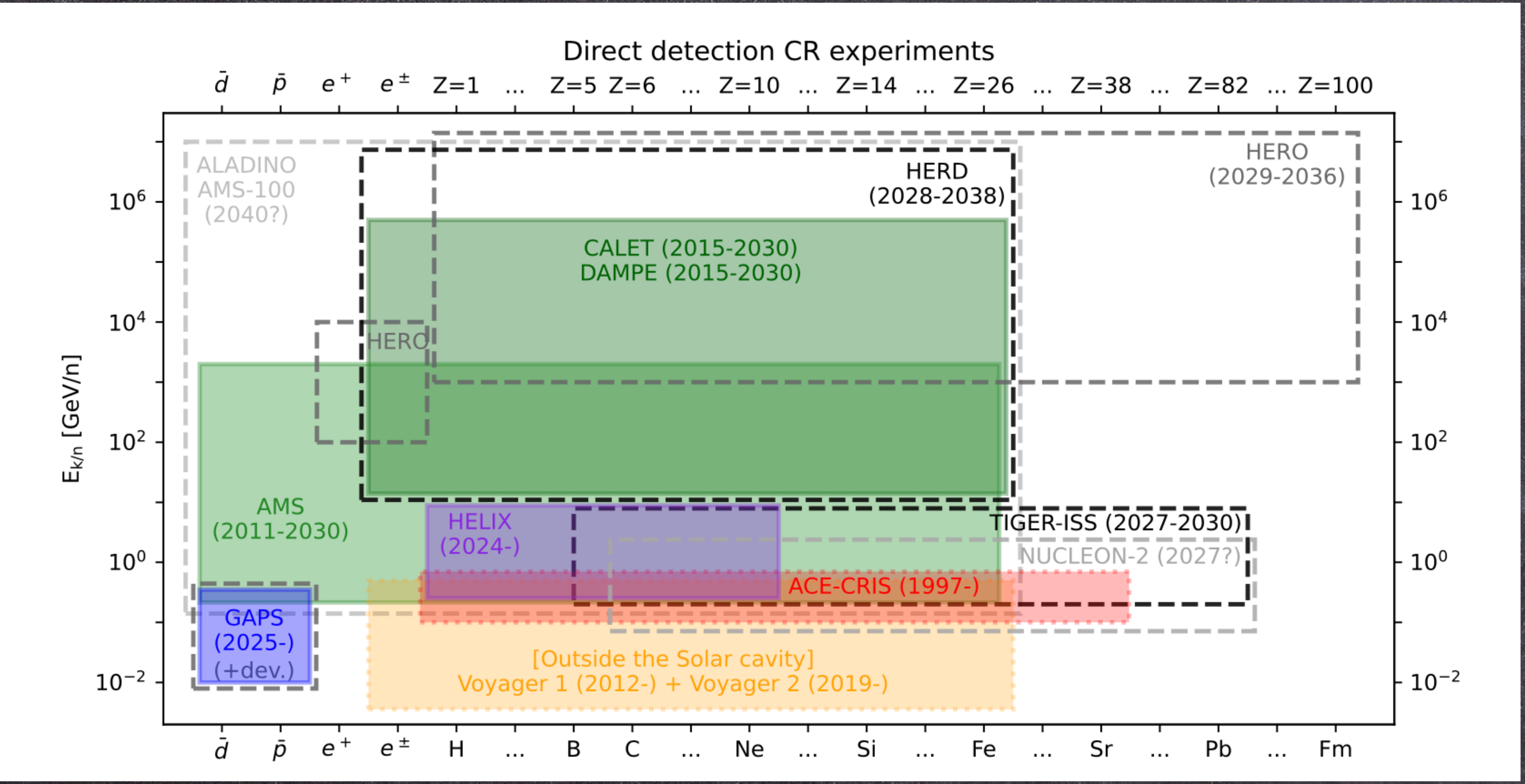

Voyager and ACE have outlasted their initial programme

AMS, CALET and DAMPE are running

Timeline of the highest energy decade and precision data on CRs

D. Maurin, FD et al., 2503.16173

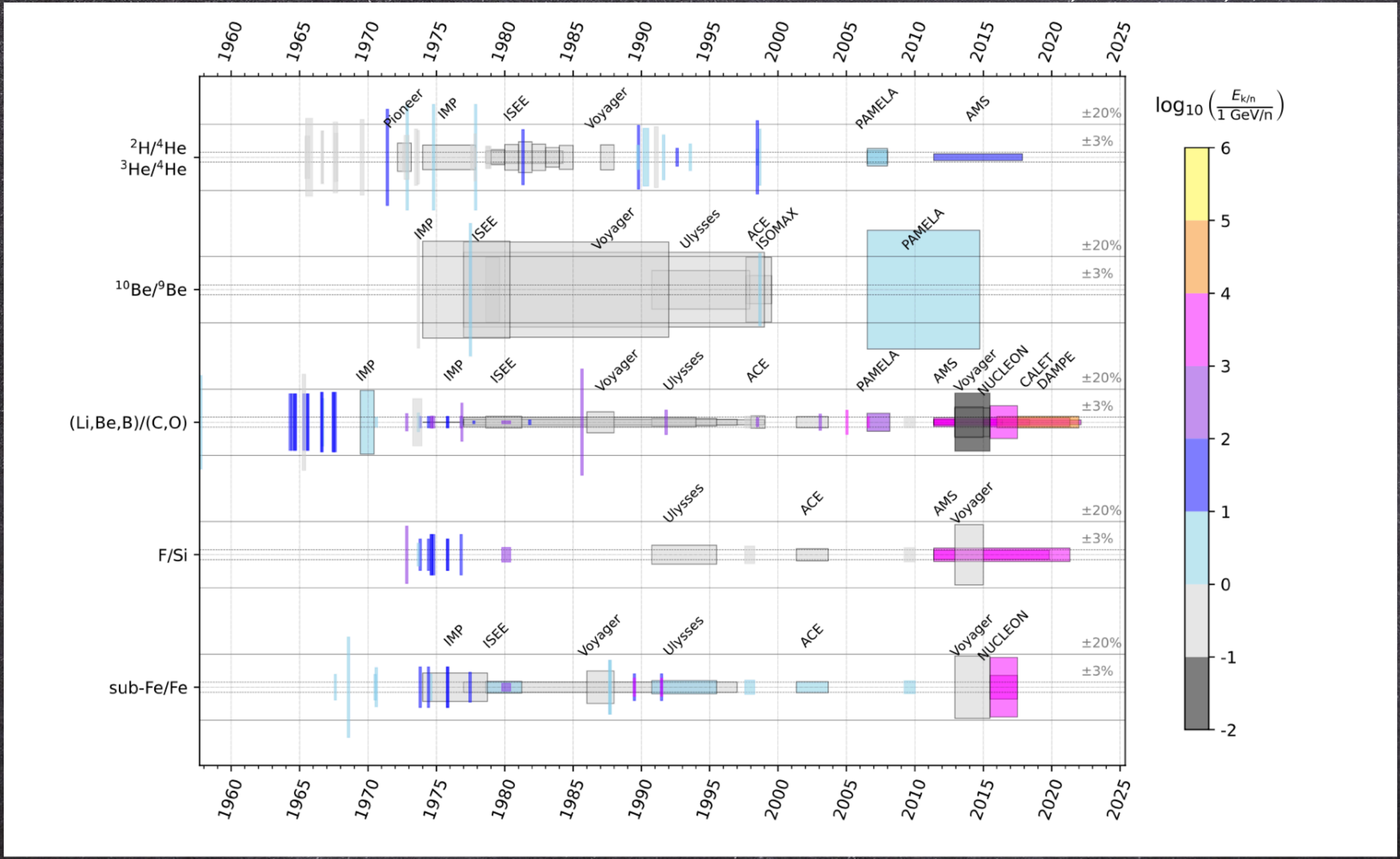

CR physics in space is precision physics

Propagation models vs data

Several propagation models are tested

Di Mauro, Korsmeier, Cuoco PRD 2024

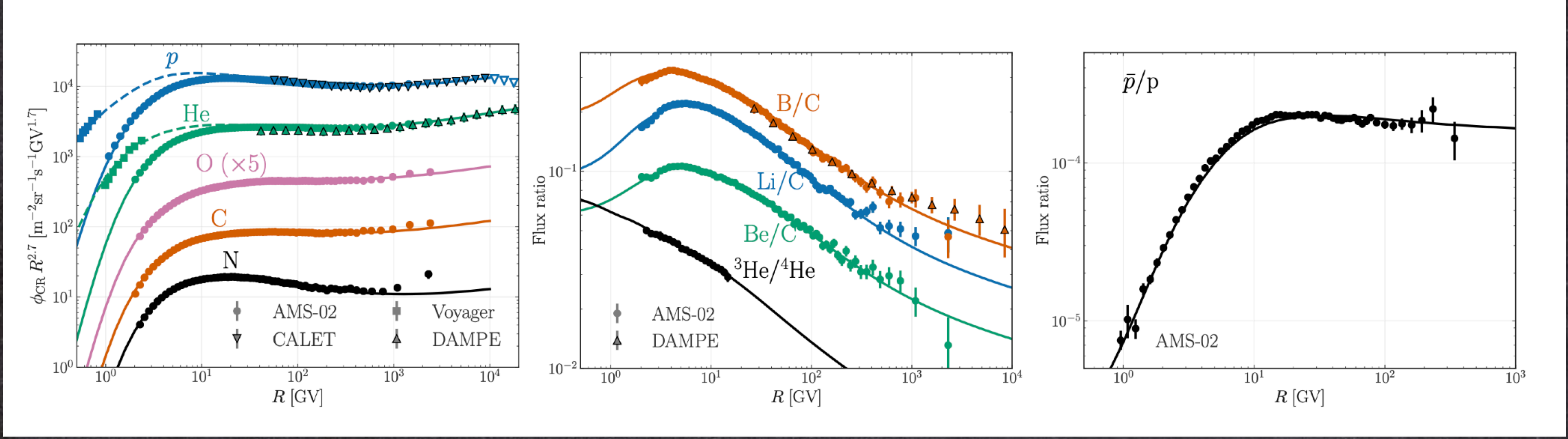

See also Weinrich+ A&A 2020, Evoli+ PRD 2020; Schroer+ PRD 2021; Cuoco&Korsmeier PRD 2021, 2022

Data on nuclear species are well described by propagation models with diffusion coefficient power index δ = 0.50 ± 0.03.

Interpretation hampered by cross sections

Cross sections for Galactic CRs: a step forward

https://indico.cern.ch/event/1377509/ @ CERN, 10/2024

(D. Maurin, FD, S. Mariani)

Precision cross-sections for advancing cosmic-ray physics and other applications: a comprehensive programme for the next decade

D. Maurin[a,*], L. Audouin[b], E. Berti[c], P. Coppin[d], M. Di Mauro[e], P. von Doetinchem[f], F. Donato[e,g,h], C. Evoli[i,j], Y. Génolini[k], P. Ghosh[l], I. Leya[m], M. J. Losekamm[n,o], S. Mariani[h], J. W. Norbury[p], L. Orusa[q,r], M. Paniccia[d], T. Poeschl[h], P. D. Serpico[k], A. Tykhonov[d], M. Unger[s], M. Vanstalle[t], M.-J. Zhao[u,v], D. Boncioli[w,j], M. Chiosso[e,g], D. Giordano[e], D. M. Gomez Coral[x], G. Graziani[c], C. Lucarelli[h], P. Maestro[y,z], M. Mahlein[n], L. Morejon[aa], J. Ocampo-Peleteiro[ab], A. Oliva[ab], T. Pierog[t], L. Šerkšnytė[h]

D. Maurin et al. 2503.16173, subm. to Physics Report

Sources of $e^{\pm}$

Secondary e+ production channels

$$q_{ij}(T_{e^+}) = 4\pi\, n_{\mathrm{ISM},j} \int dT_i\, \phi_i(T_i) \frac{d\sigma_{ij}}{dT_{e^+}}(T_i, T_{e^+})$$

L. Orusa, M. Di Mauro, FD, M. Korsmeier PRD 2022

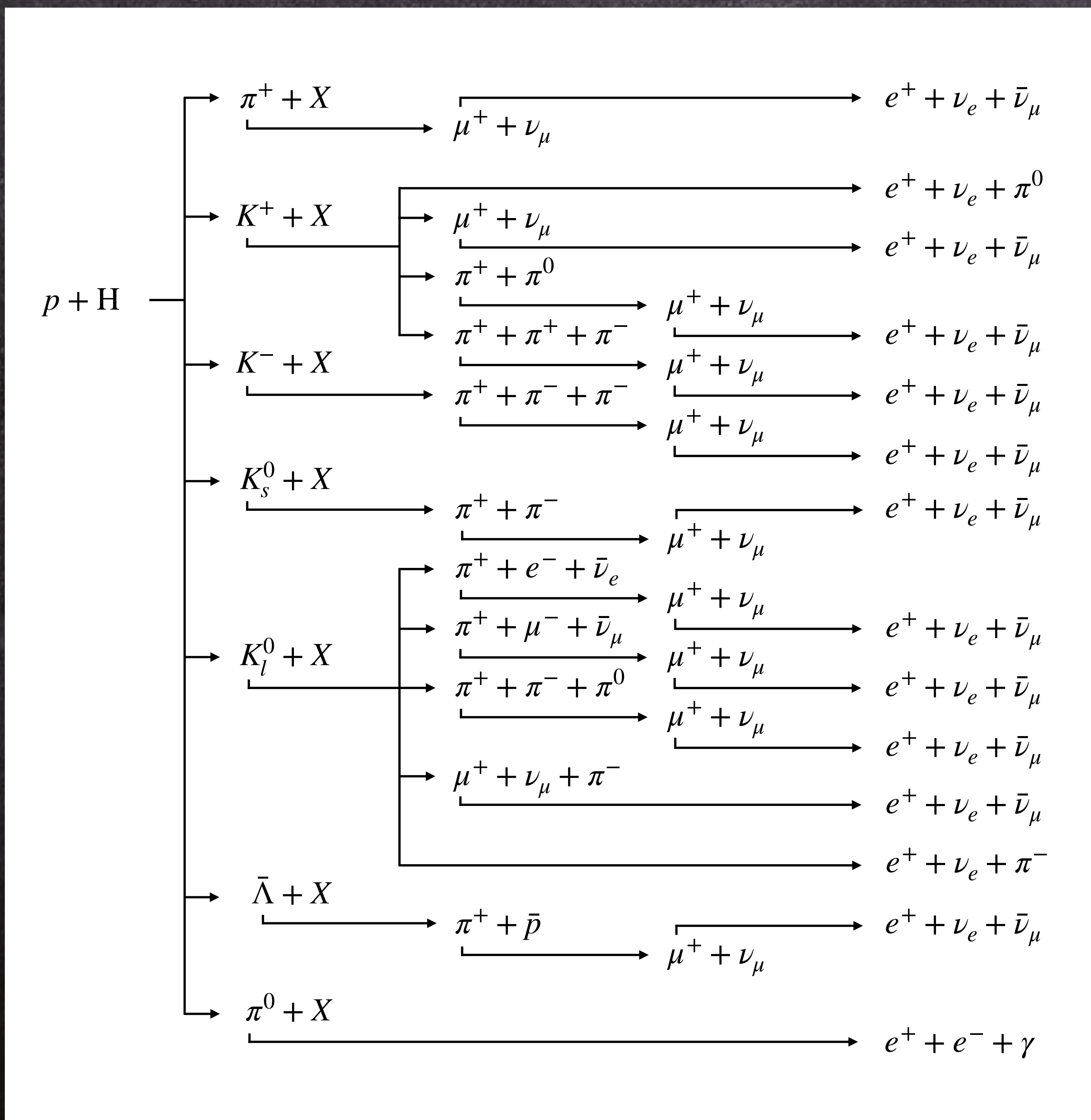

Di Mauro, FD, Korsmeier, Manconi, Orusa, PRD 2023

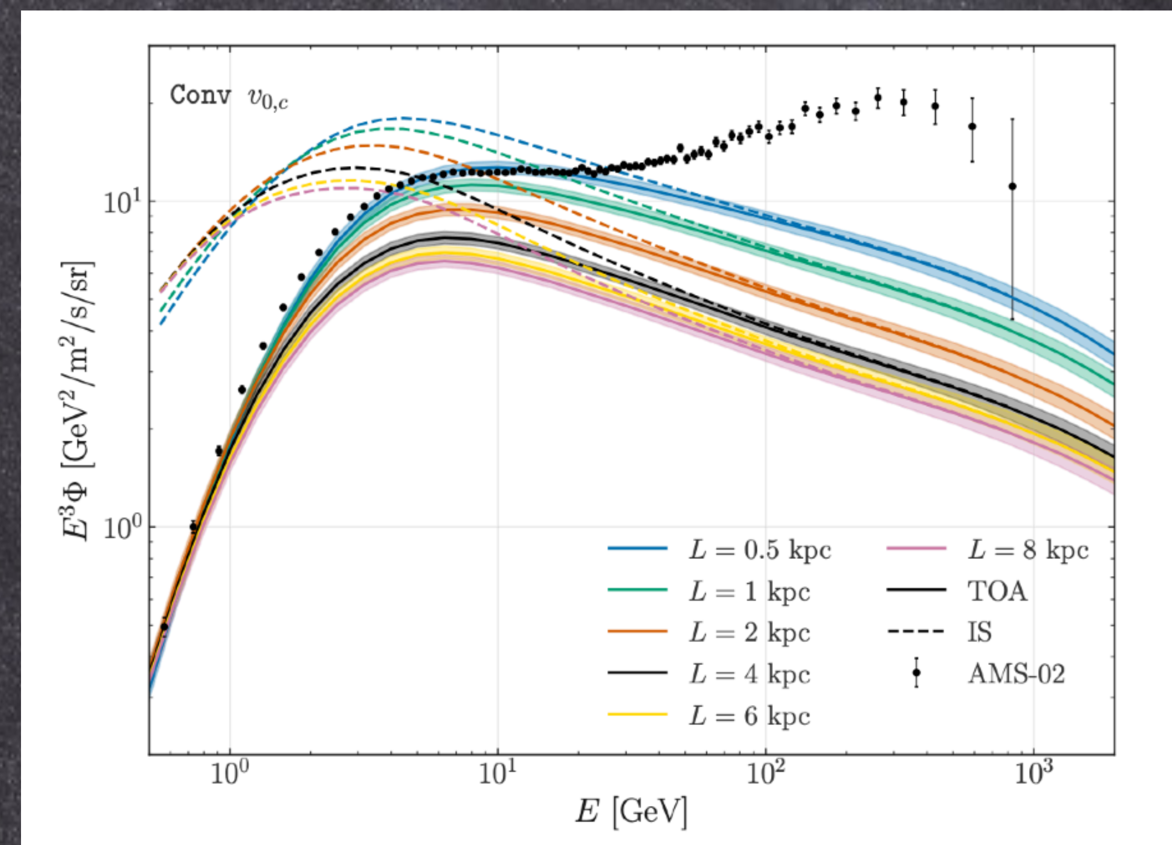

e+ secondaries contribute significantly below few GeV

Cross section uncertainties comparable to propagation ones at fixed halo size

Electrons from supernova remnants

Ellison+ ApJ 2007; Blasi 2013; Di Mauro+ JCAP 2014: Evoli+ PRD 2021;

SNR are considered the main sources of galactic CRs - nuclei from p to Fe, and e-

Manconi, Di Mauro, FD JCAP2017; JCAP 2019

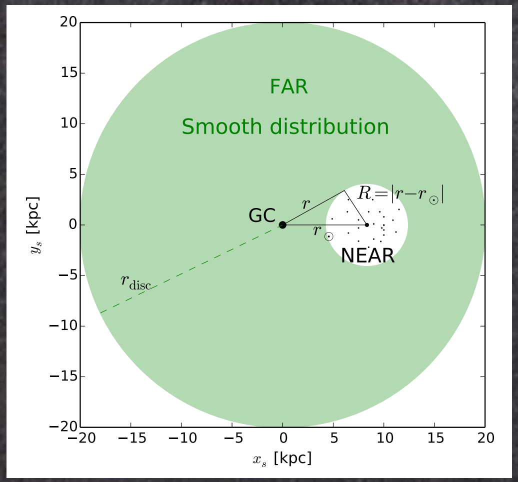

- Hadronic acceleration: evidence of π^0 bump (Fermi-LAT+ 2010)
- Leptonic acceleration: evidence of synchrotron emission in radio and X-rays

Injection spectrum:

$$Q(E) = Q_0 \left(\frac{E}{E_0}\right)^{-\gamma} \exp\left(-\frac{E}{E_c}\right)$$

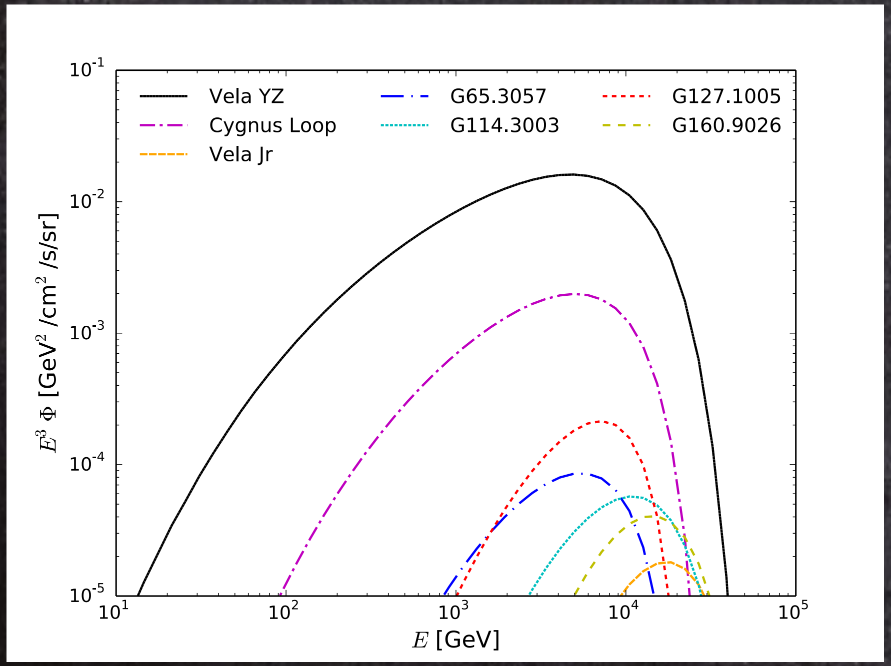

e- flux from near SNR (Vela XY and Cygnus Loop at d<0.5 kpc)

Few SNR can contribute to TeV flux

Additional e- from a smooth SNR distribution

e± from Pulsars (PWN)

High magnetic fields (10^9–10^{12} G) extract wind of e- from the pulsar surface, e± pairs produced in EM cascades

Pulsar spin-down energy (W_0) is transferred to e± pairs, accelerated to very high energy with $Q \sim E^{-\gamma}$.

After several kyrs e± can be released in the ISM

These e± pairs radiate by Inverse Compton scattering and synchrotoron radiation, and shine at many frequencies

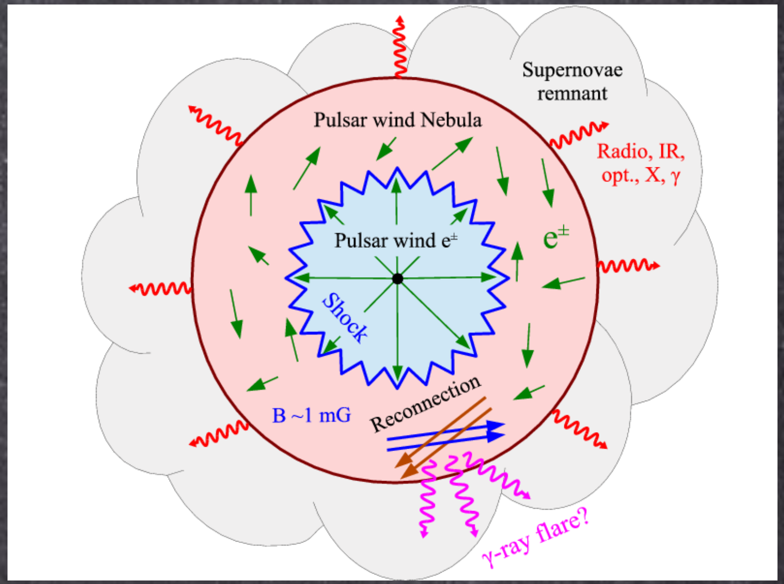

$$E_{\rm tot} = \eta W_0 = \int_0^T dt \int_{E_1}^{\infty} dE E Q(E,t)$$

The total energy E_{tot} emitted in e± by a PWN is a fraction η (efficiency conversion) of the spin-down energy W_0. Relevant parameters: γ and η

e+ & e- spectra, a natural explanation

e+ and e- AMS-02 spectra fitted with a multi-component model:
secondary production, e- from SNR, e+ from PWN

Di Mauro, FD, Manconi PRD 2021

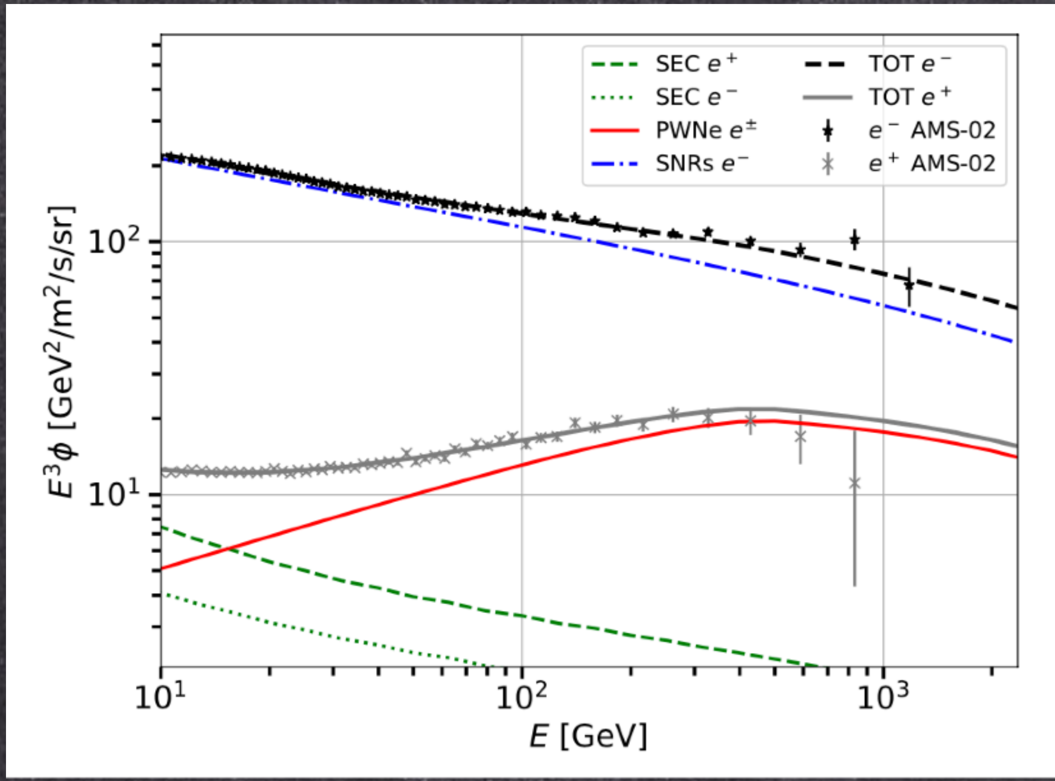

No need to add exotic (DM) sources, Sec+PWN do the job

(Hooper+2009; Grassi+2009; Delahaye+2010;Di Mauro, FD+2014, Orusa+ 2023... many others)

The break at 42 GeV in e- is explained by interplay between SNR and PWN

See also Fang+ 2007. 15601, Evoli+PRD 2021, Cuoco+ PRD2020

Simulation of Galactic pulsar populations: a fit to AMS-02 e+ data

L. Orusa, S. Manconi, M. Di Mauro, FD JCAP 2021

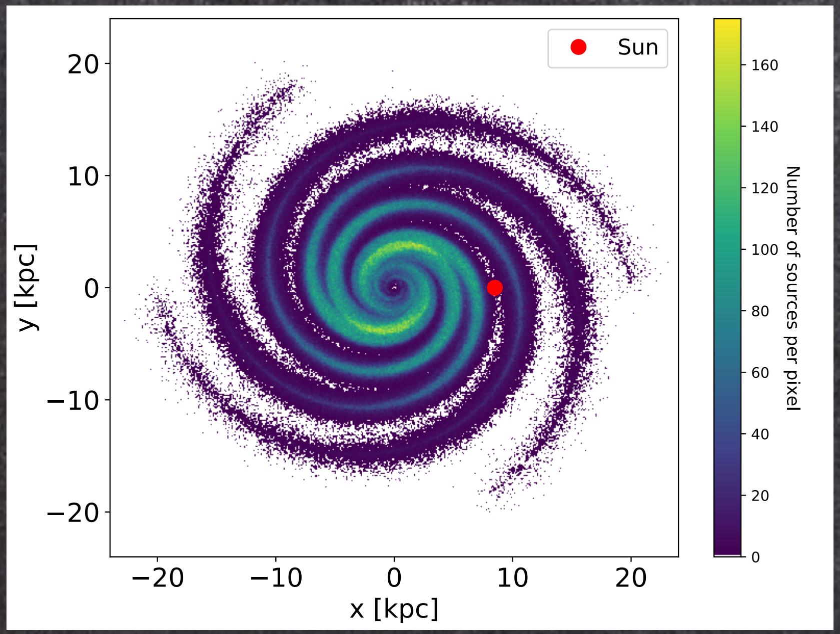

- Simulation of space distribution and pulsar properties
- The contribution of pulsars to e+ is dominant above 100 GeV
- May have different features
- E>1 TeV: unconstrained by data
- Secondaries forbid evidence of sharp cut-off
- No need for Dark matter, indeed

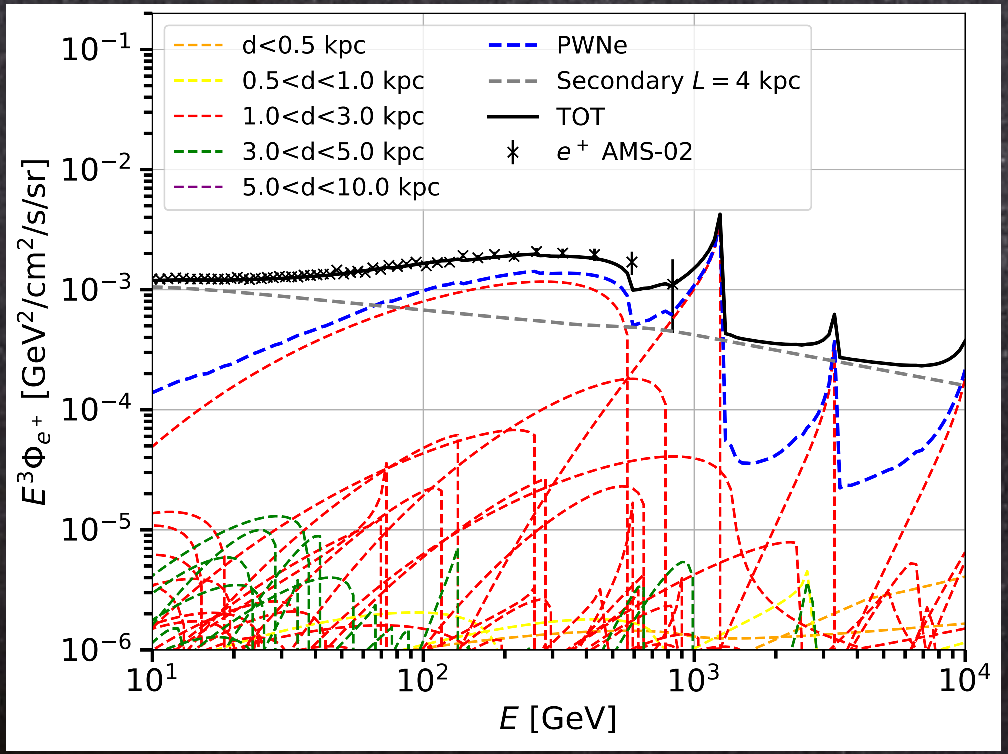

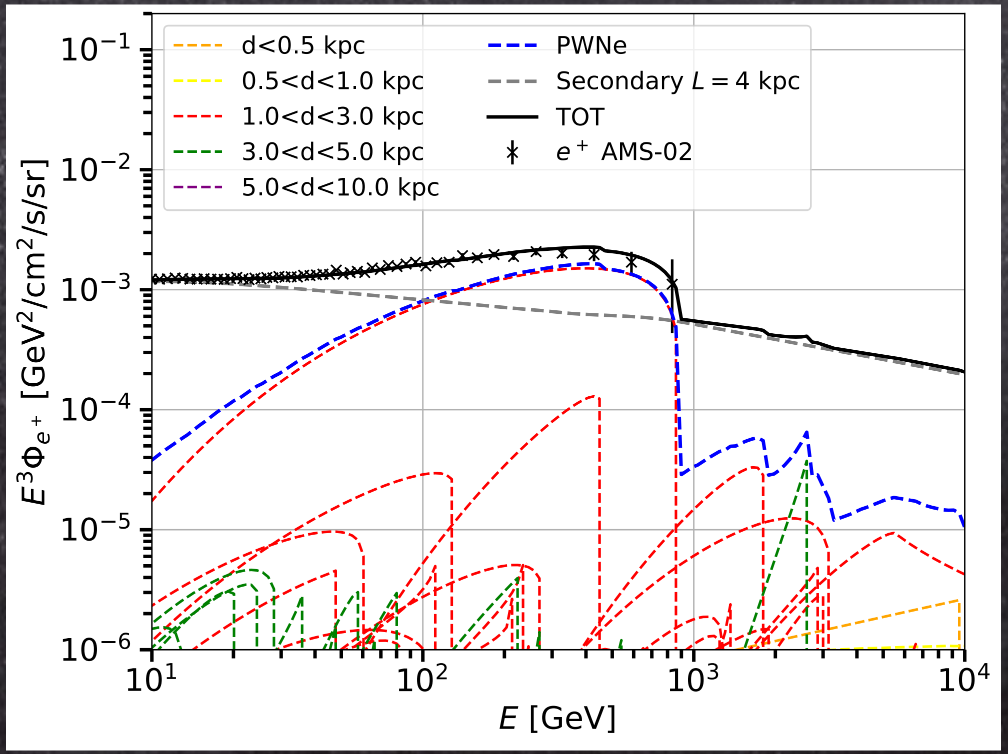

Simulations: effect of age and distance

on mock galaxies as selected by e+ AMS-02 data

L. Orusa, S. Manconi, M. Di Mauro, FD JCAP 2021

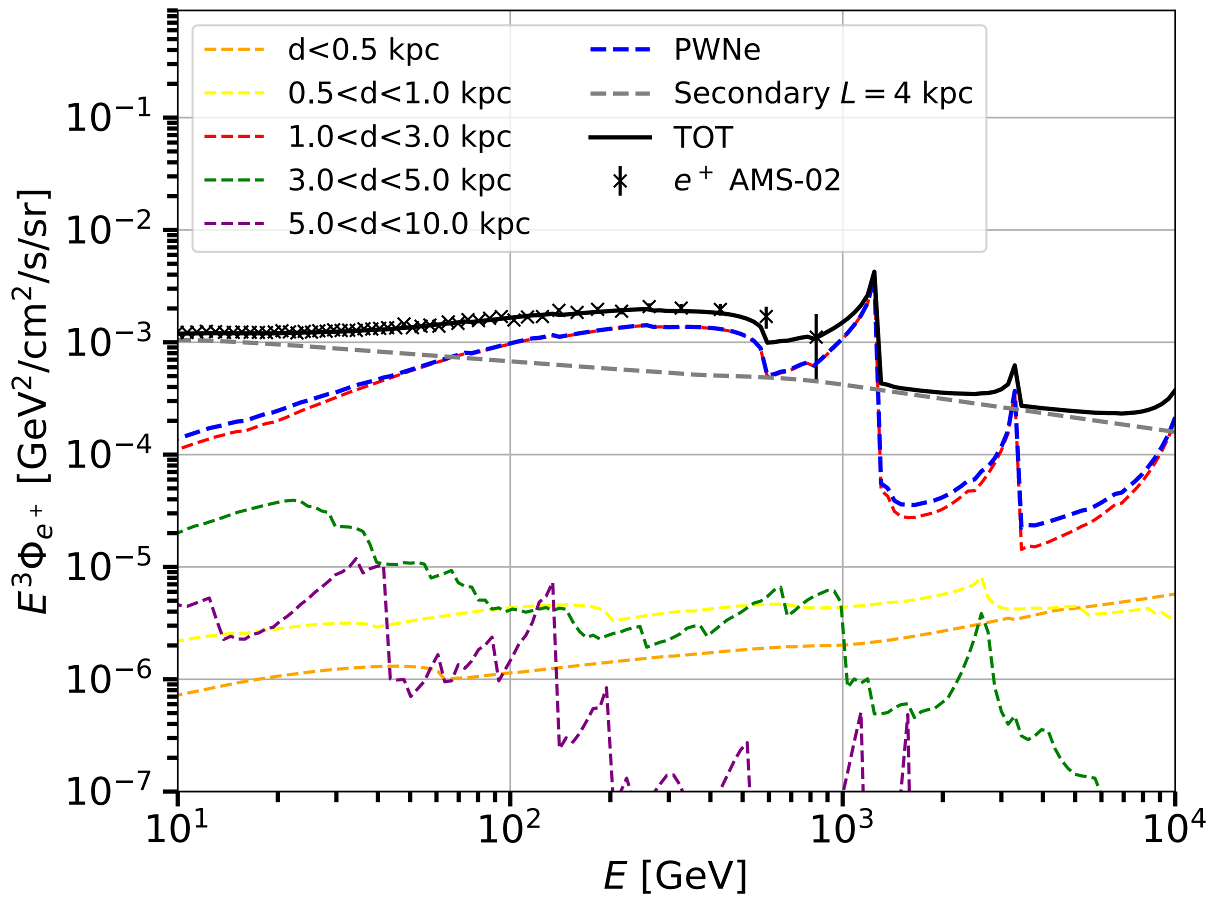

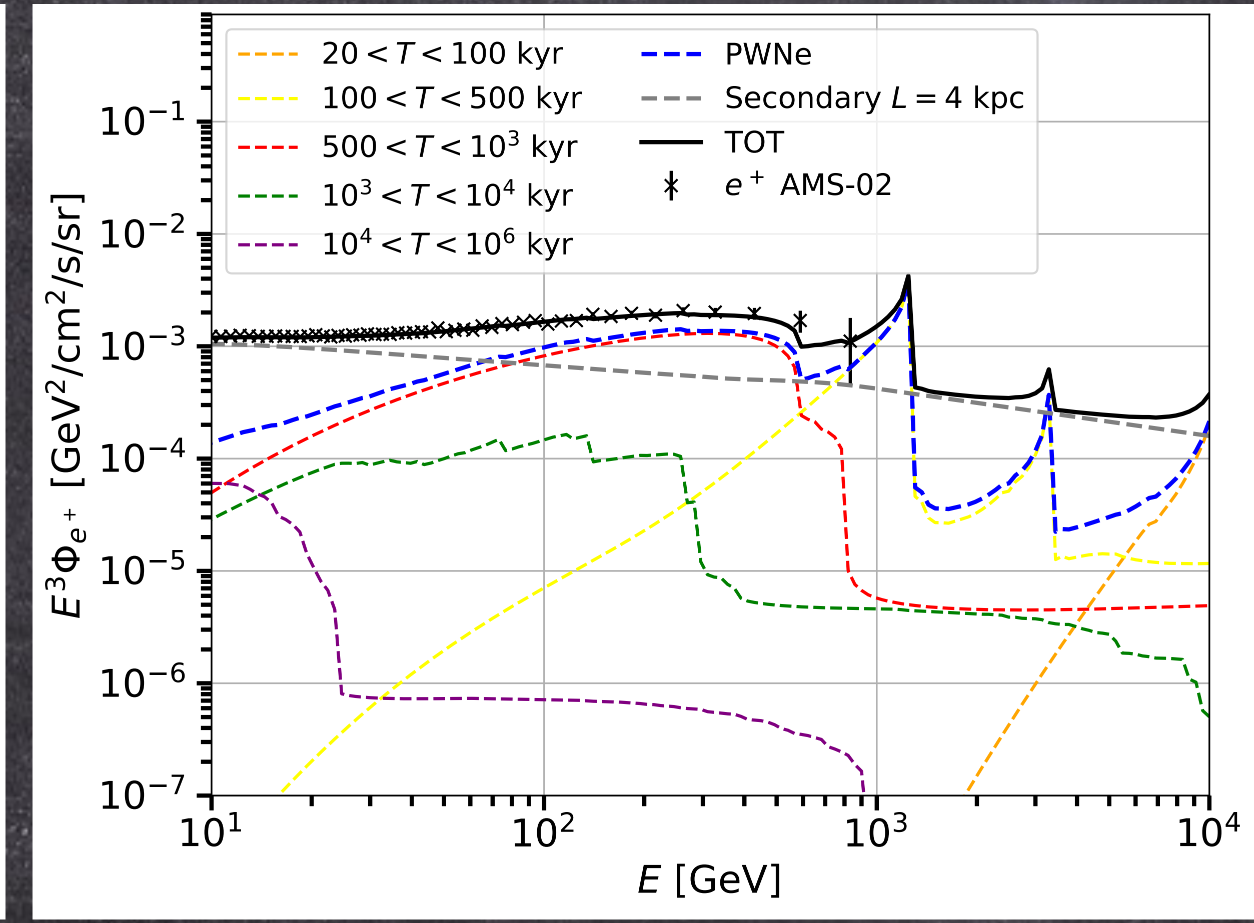

1-3 kpc ring is the most fruitful in terms of e+

Interplay between spiral arms and propagation length

Few pulsars suffice to fit AMS data

Very few ones, indeed

L. Orusa, S. Manconi, M. Di Mauro, FD JCAP 2021

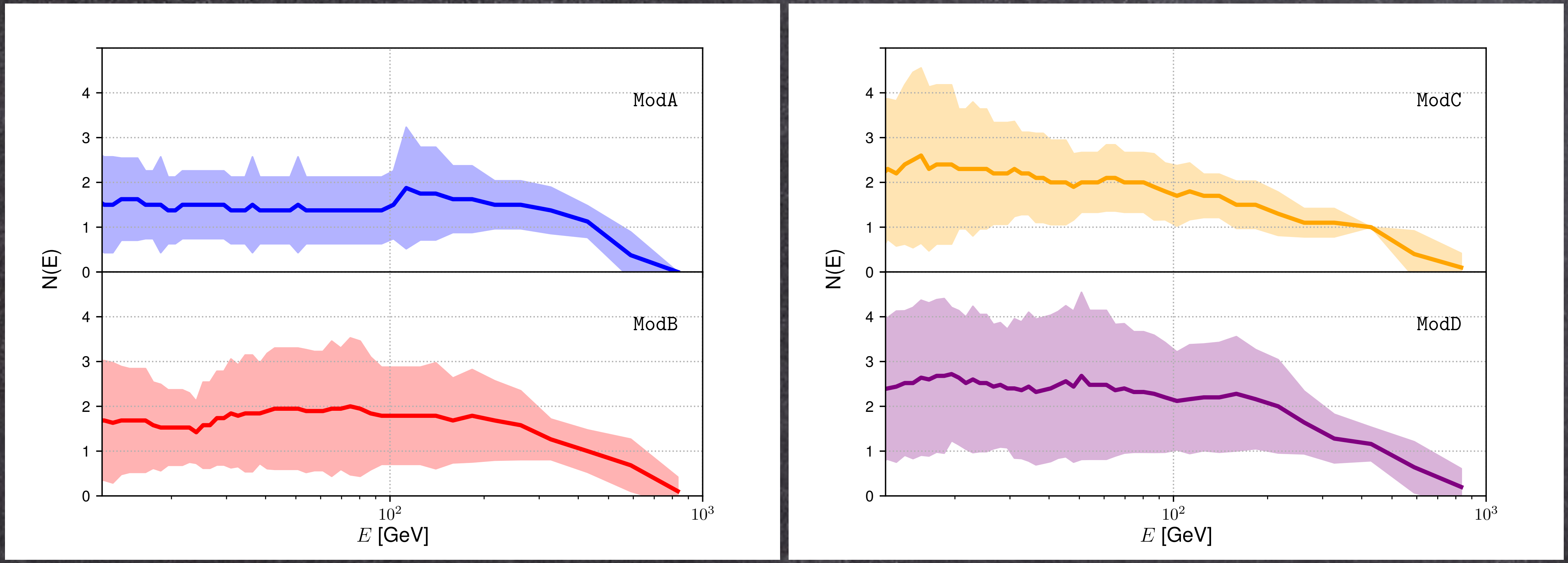

N(E) is the mean number of PWNe that produce a flux higher than the experimental flux error in at least one energy between above 10 GeV.

<u>Typically 2-3 sources explain most of the measured flux (+ secs)</u>

e± pair emission from pulsars

We assume continuous injection :

$$Q(E,t) = L(t)\left(\frac{E}{E_0}\right)^{-\gamma_e} \exp\left(-\frac{E}{E_c}\right) \qquad L(t) = \frac{L_0}{\left(1+\frac{t}{\tau_0}\right)^{\frac{n+1}{n-1}}}$$

Normalized to:

$$E_{tot} = \eta W_0 = \int_0^T dt \int_{E_1}^{\infty} dE E Q(E,t)$$

Having:

$$\dot{E} = \frac{dE_{\rm rot}}{dt} = I\Omega\dot{\Omega} = -4\pi^2 I \frac{\dot{P}}{P^3}\,.$$

We can derive a relation for:

$$\tau_0 = \frac{P_0}{(n-1)\dot{P}_0}.$$

Positrons form catalogued pulsars

L. Orusa, M. Di Mauro, FD, S. Manconi 2024, JCAP 2024

We pick pulsars from the ATNF catalog: position, age, dE/dt

The other pulsar parameters are simulated (see Orusa, Manconi, Di Mauro, FD JCAP 2021)

Propagation in the Galaxy treated according to latest nuclei results

(see Di Mauro, FD, Korsmeier, Manconi, Orusa PRD 2023)

ModA: τ_0 distribution

ModB: τ_0 fixed

ModC: delayed emission

ModD: two-zone diffusion

Pulsar property	Simulated quantity	Benchmark	Variations
Spin-down		CB20[36]	$\tau_0 = 10$ kyr
	P_0	Gaussian [0.3s; 0.15s]	-
	$\log_{10}(B)$	Gaussian [12.85G; 0.55G]	-
	n	Uniform [2.5-3]	-
	$\cos\alpha$	Uniform [0-1]	-
$e^{\pm}$ injection	γ_L	Uniform [1.0-2.0]	-
	γ_H	Uniform [2.0-2.8]	-
	E_b	Uniform [300-600] GeV	-
	η	Uniform [0.01-0.1]	-
Kick velocity	v_k	-	FK06VB [57]

Catalogued pulsars: a fit to e+ data

L. Orusa, M. Di Mauro, FD, S. Manconi JCAP2024

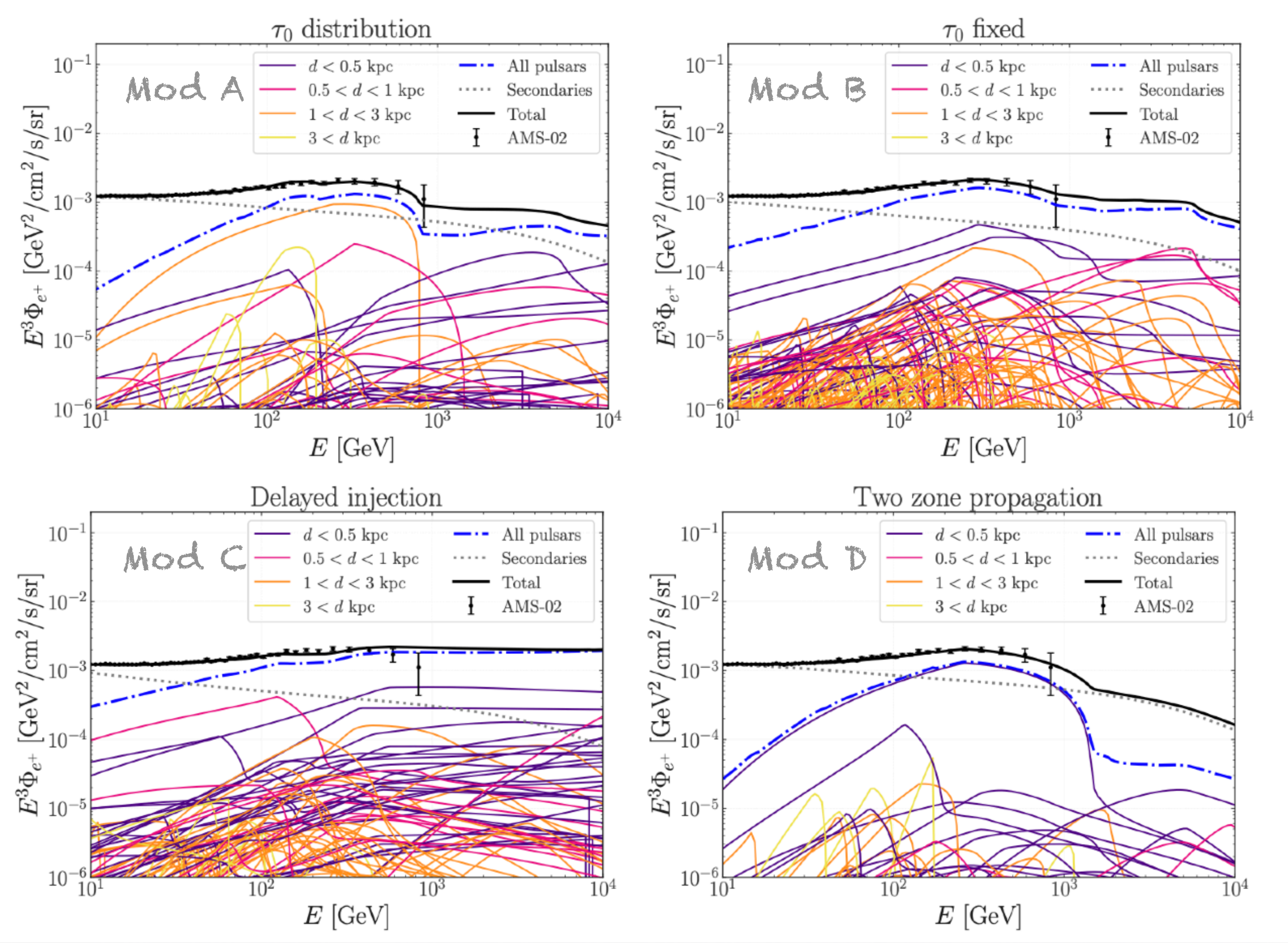

Exemplary best fits in Mod A-B-C-D

Catalogue pulsars & secondaries explain well the data.

Fixed τ_0 (Mod B) prevents scenarios with one dominant pulsar

e± from the 10 most relevant ATNF pulsars

L. Orusa, M. Di Mauro, FD, S. Manconi JCAP2024

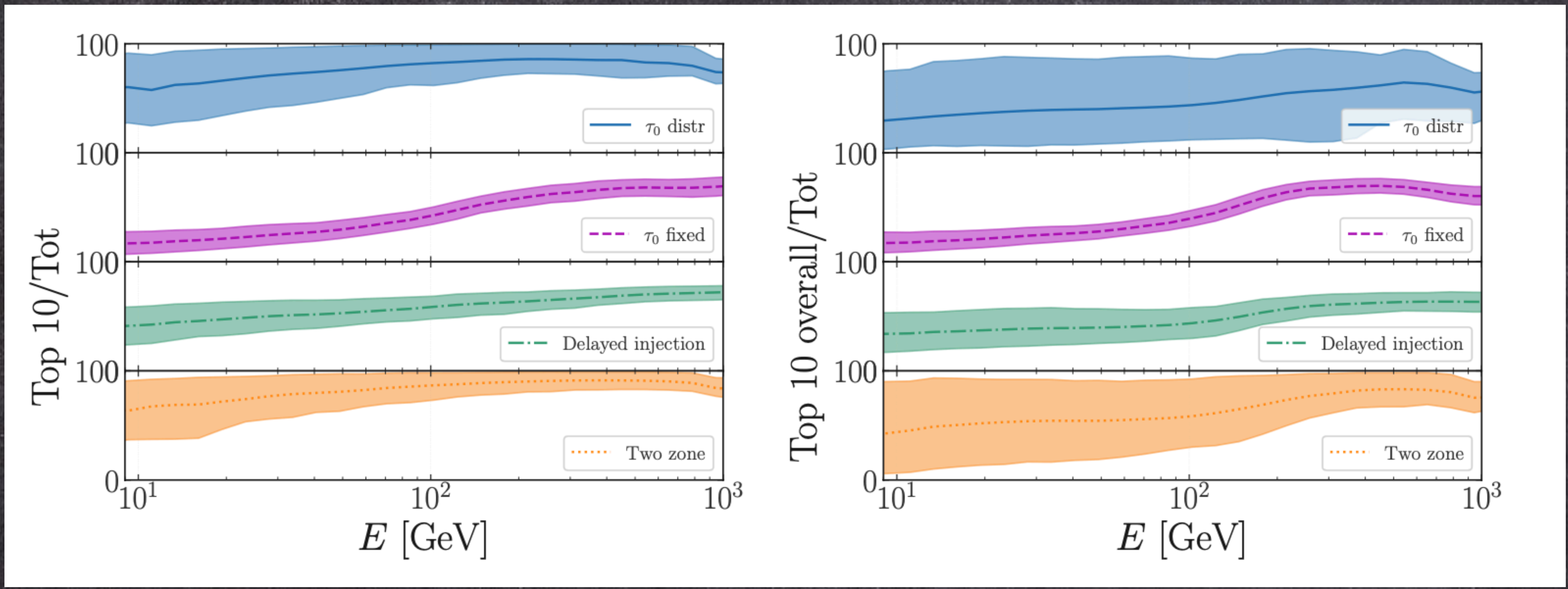

The average flux percentage produced by the top 10 brughtest sources in each realization that fits AMS-02 data (left), relative to the total flux from all pulsars.
Right: the top 10 brightest sources
For E> 100 GeV, few PSR explain > 50% of the total flux

Predictions and the data

L. Orusa, M. Di Mauro, FD, S. Manconi JCAP2024

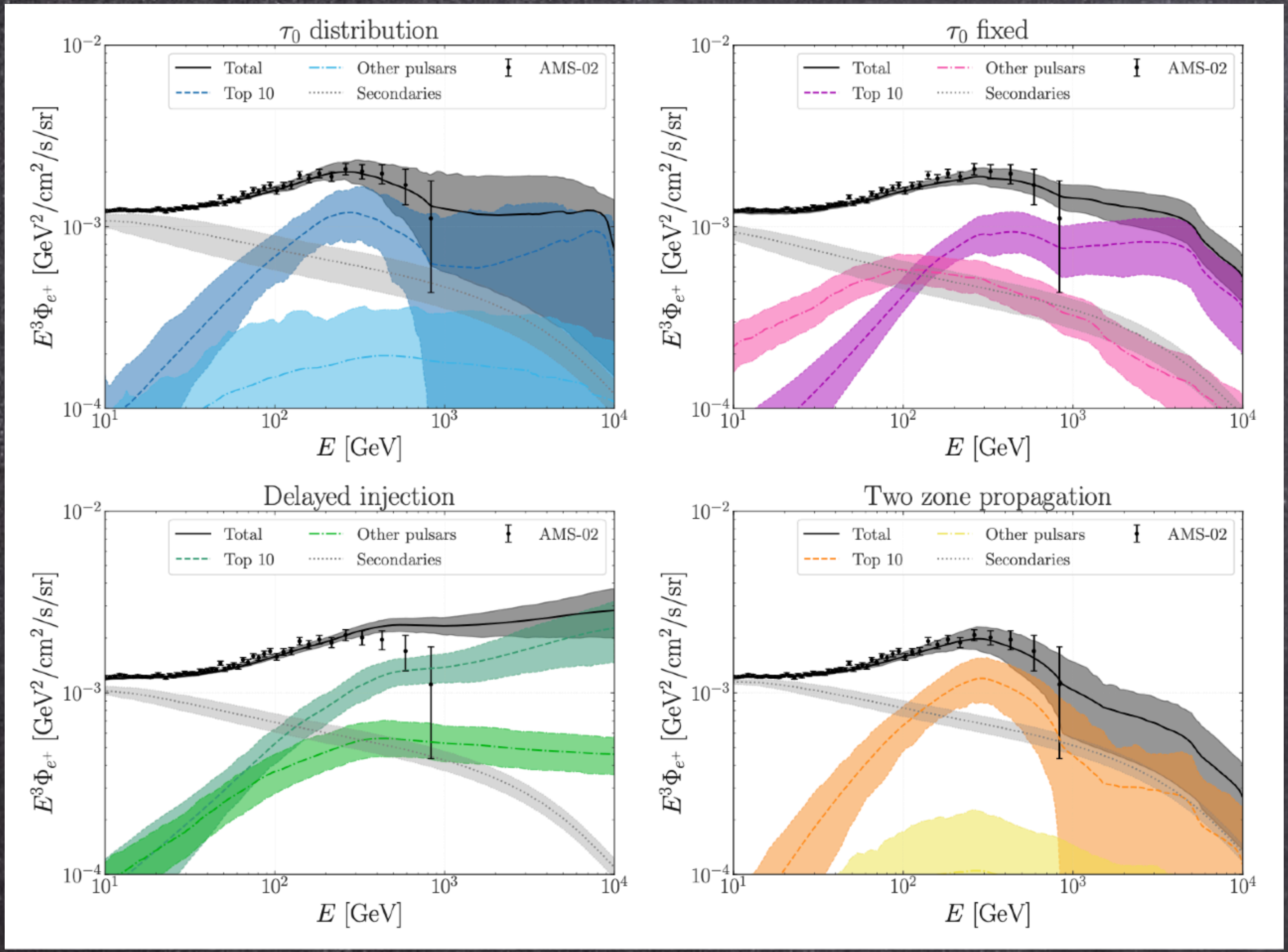

Emission models and parameters are very relevant.
Some models are predictive also above TeV.
Secondaries are allowed with a free normalization (always found < 1.5, typically around 1)

γ -ray halos around pulsars

HAWC detections of γ-ray haloes around pulsars

Extended haloes have been detected by HAWC around Geminga and Monogem, and by Lhaaso around PRS J0622+3749

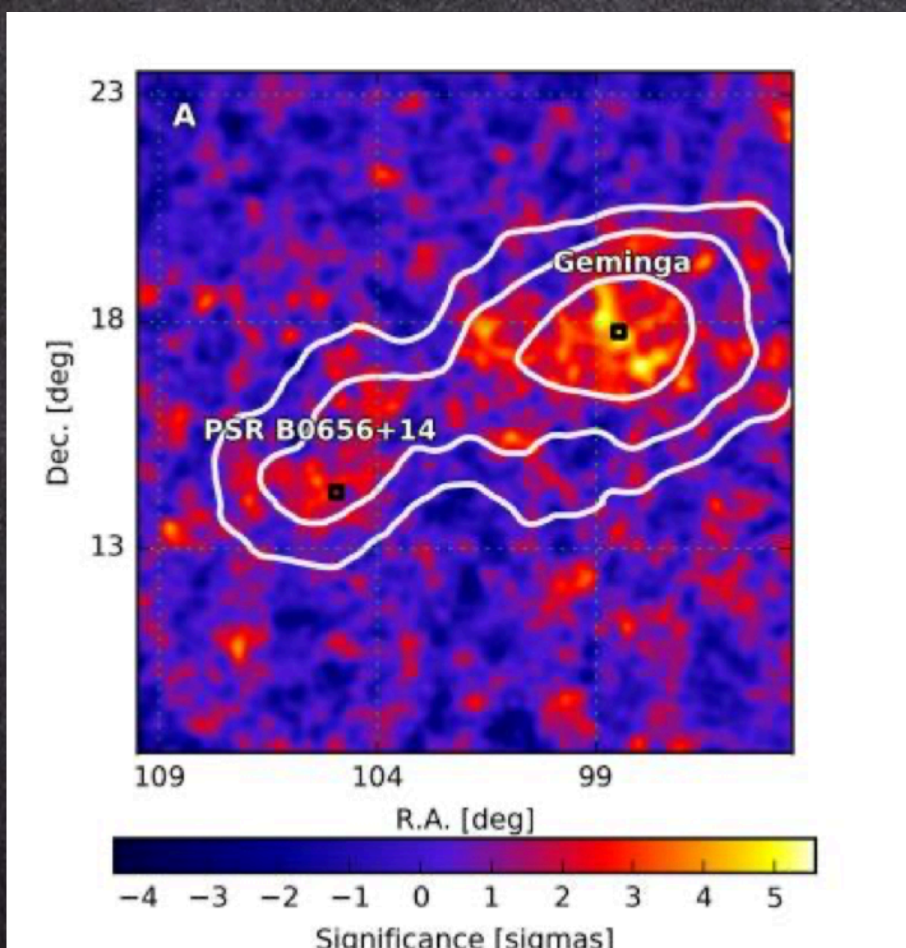

HAWC Collaboration, Sience 2017

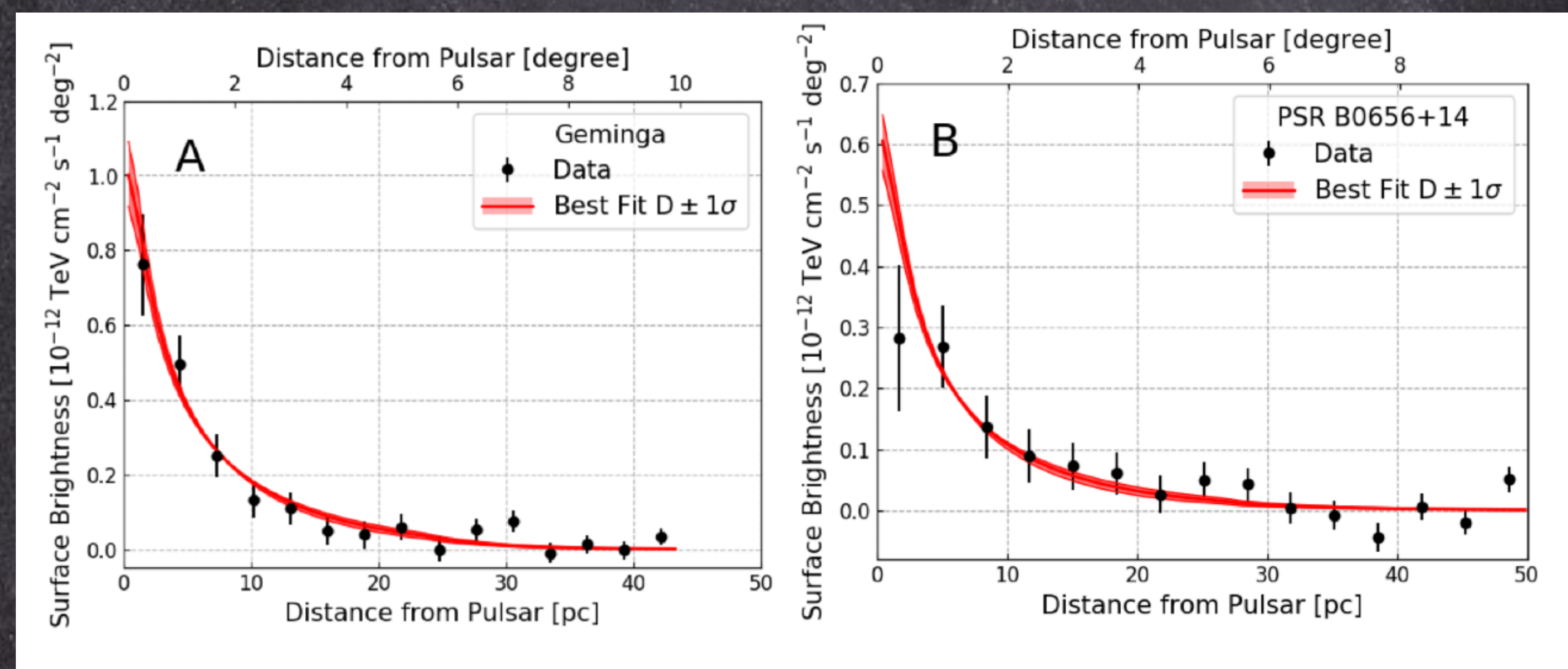

Interpreted as γ-rays from Inverse Compton scattering

Inverse Compton scattering power

M. Di Mauro, S. Manconi, M. Negro, FD, PRD 2021

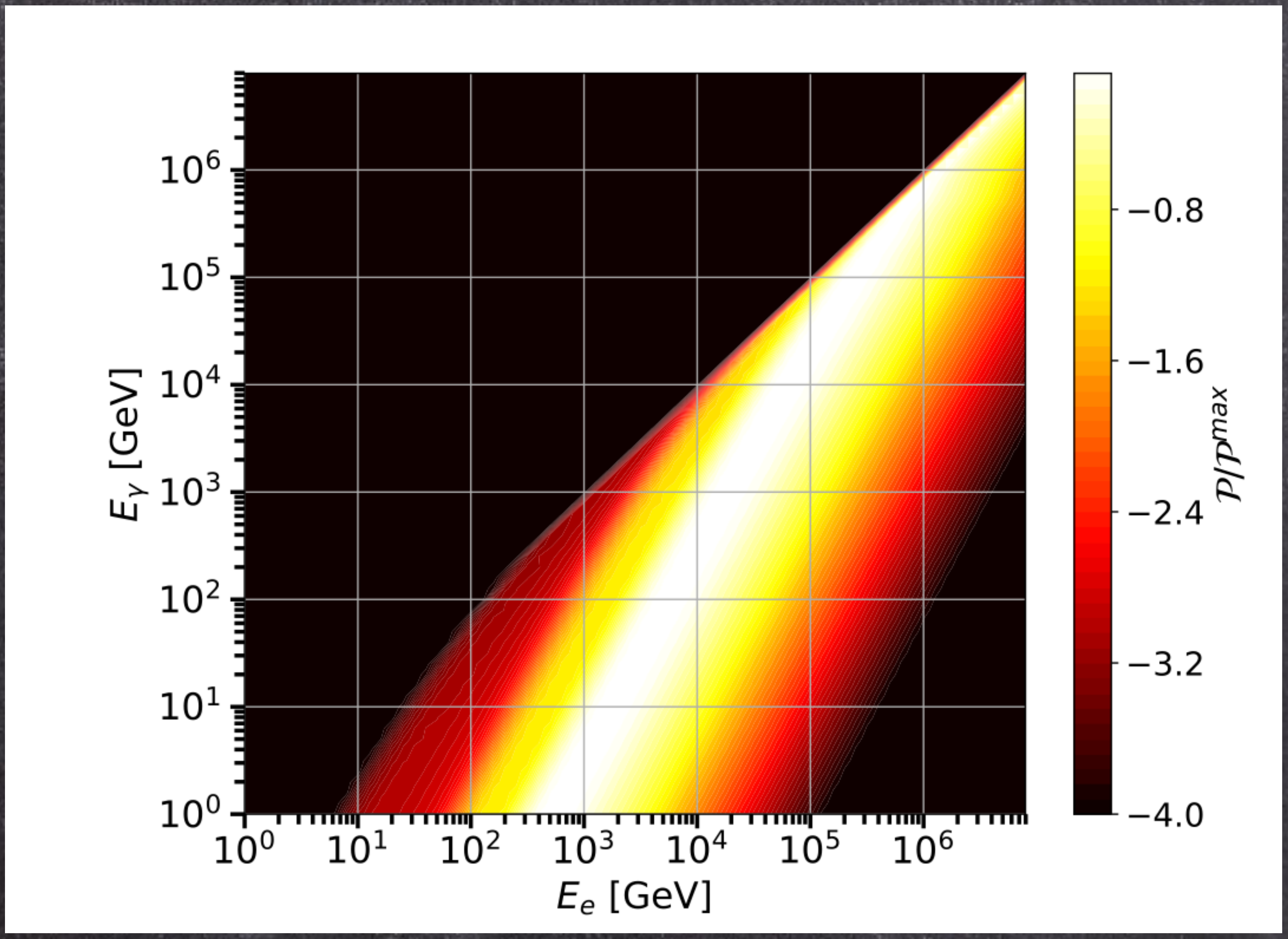

The γ-rays are 5-60 times less energetic than parent leptons
HAWC γ-rays probe electrons with 100-1000 TeV

Discovery of Geminga γ-ray halo in Fermi-LAT data

M. Di Mauro, S. Manconi, FD, PRD 2019

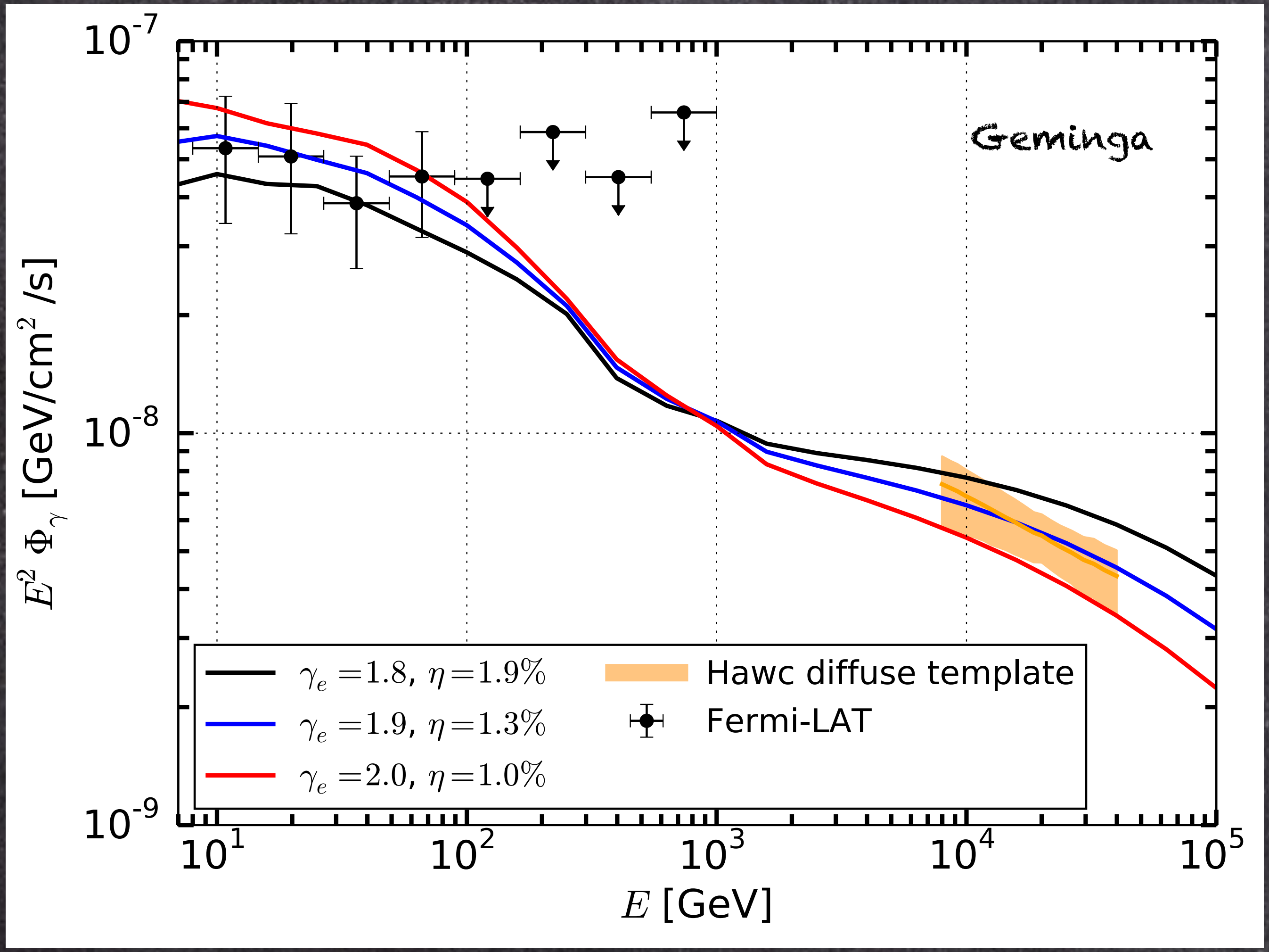

M. Di Mauro, S. Manconi, M. Negro, FD, PRD 2021

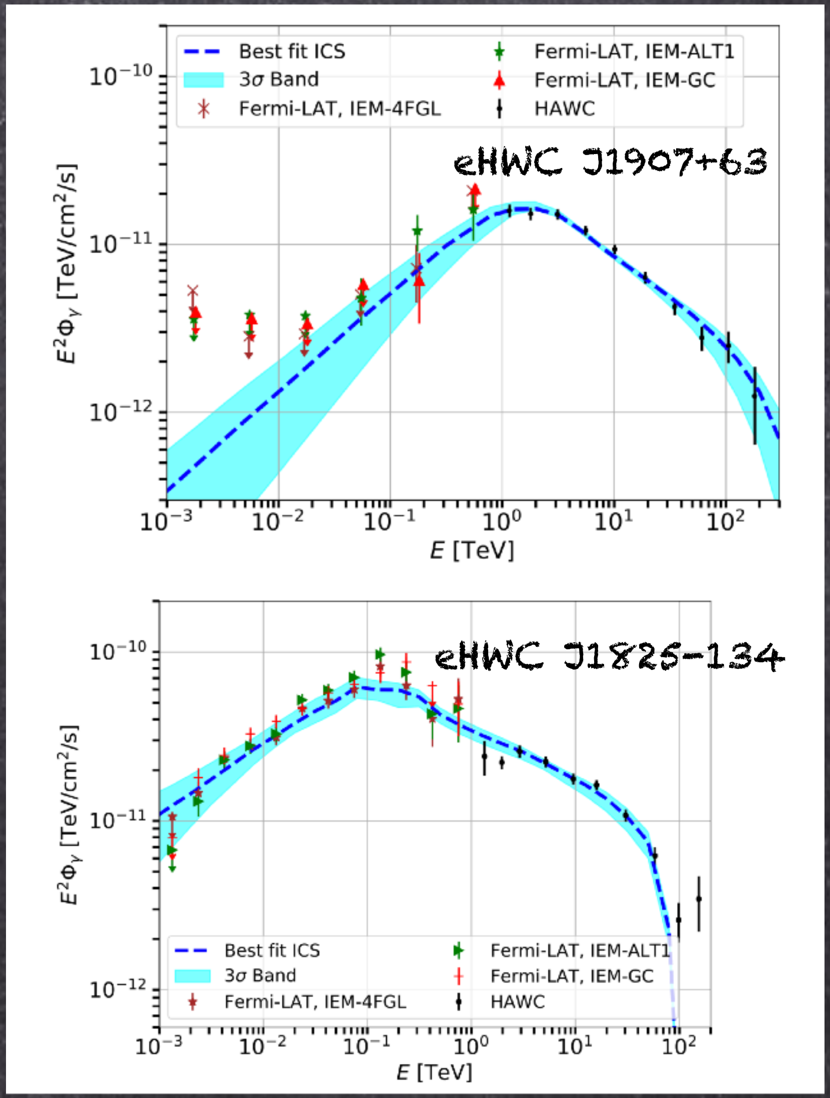

Interpreted as γ-rays from Inverse Compton scattering

For a review on γ-ray haloes around pulsars: Amato&Recchia 2409.00659

Detections of γ-ray haloes around pulsars

Lhaaso Coll. PRL 2021

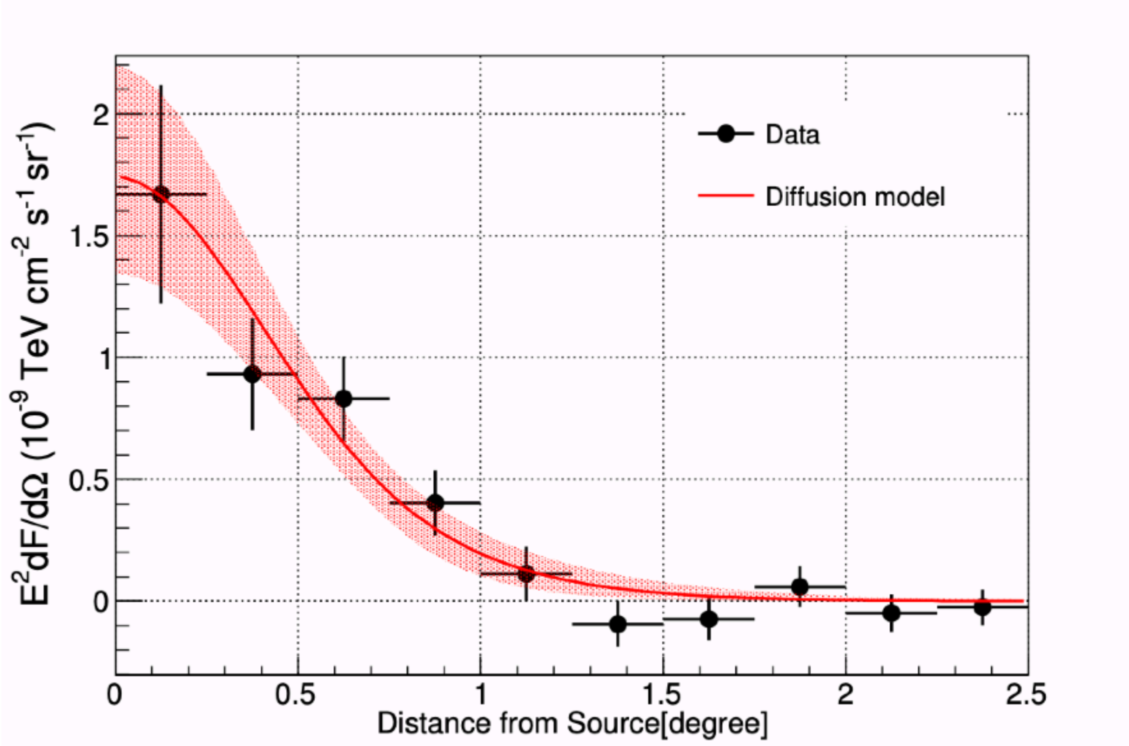

FIG. 2. One-dimensional distribution of the > 25 TeV γ-ray emission of LHAASO J0621+3755. The solid line and shaded band show the best fit and $\Delta\chi^2$ = 2.3 range of the diffusion model fit, which is the convolution of Eq. (1) with the PSF.

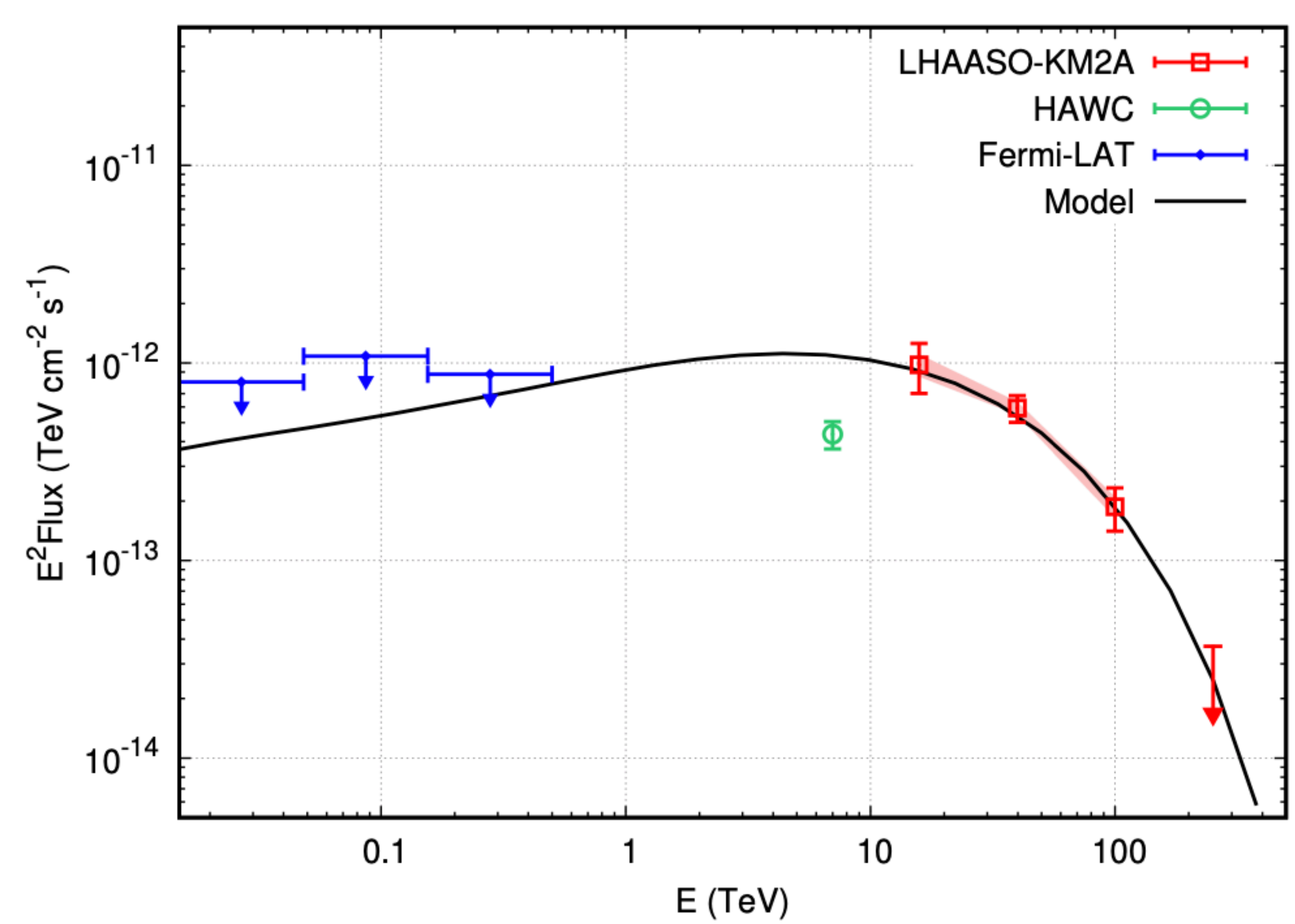

Extremely high energy γ -rays are observed around the pulsar as an extended halo. A spectrum is measured.

This new class of observations needs revisiting our understanding of acceleration of leptons to very high energies and emission of photons

Consequence of ICS Geminga halo on positron flux at Earth

M. Di Mauro, S. Manconi, FD PRD 2019

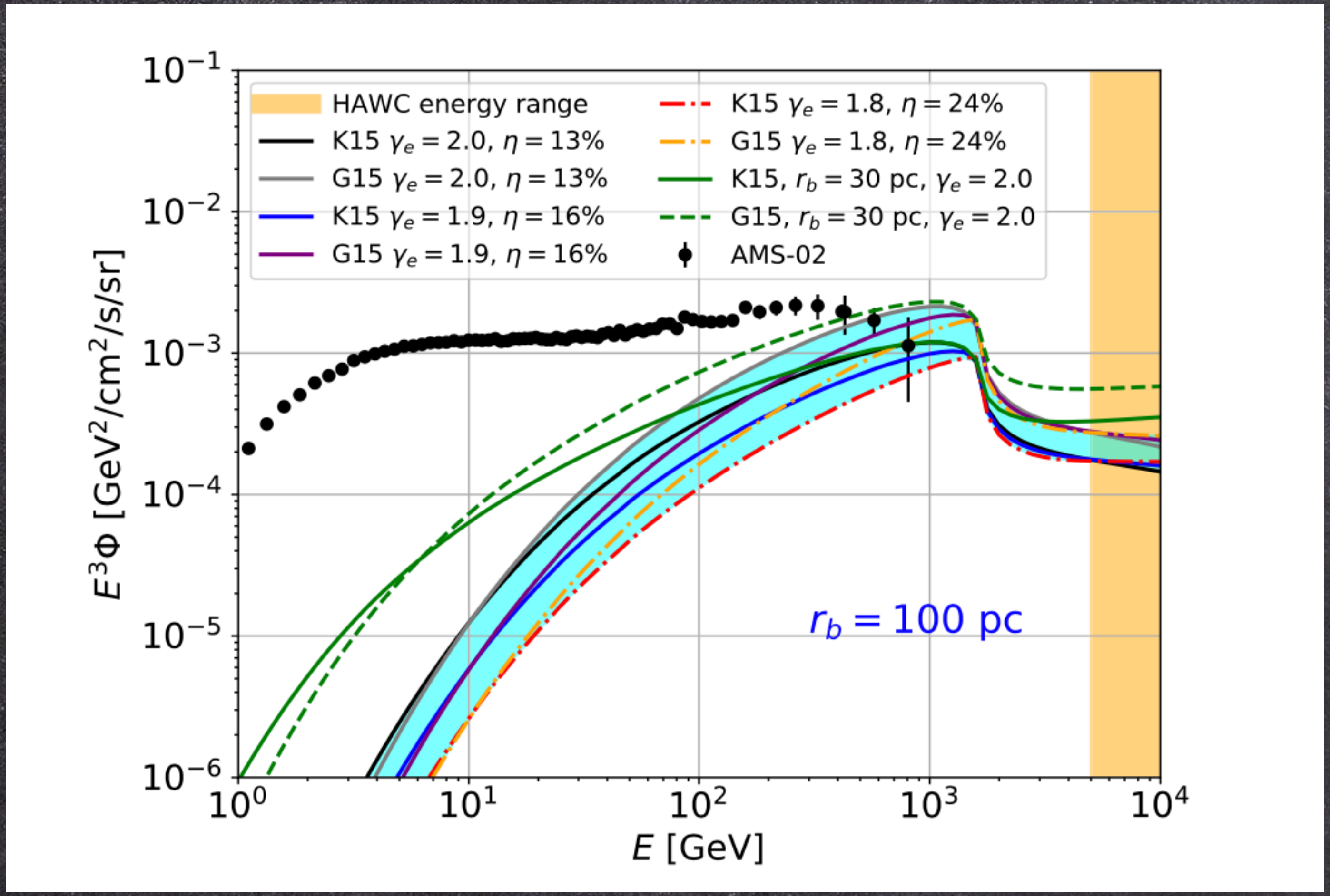

One single source as Geminga contributes significantly to high energy positrons as measured by AMS

Uncertainty in the diffusion around the source(s)

See also Schroer, Evoli, Blasi PRD 2023

Precise Measurements of γ-ray halos around Geminga and Monogem with HAWC

HAWC Coll. & M.Di Mauro ApJ 2025

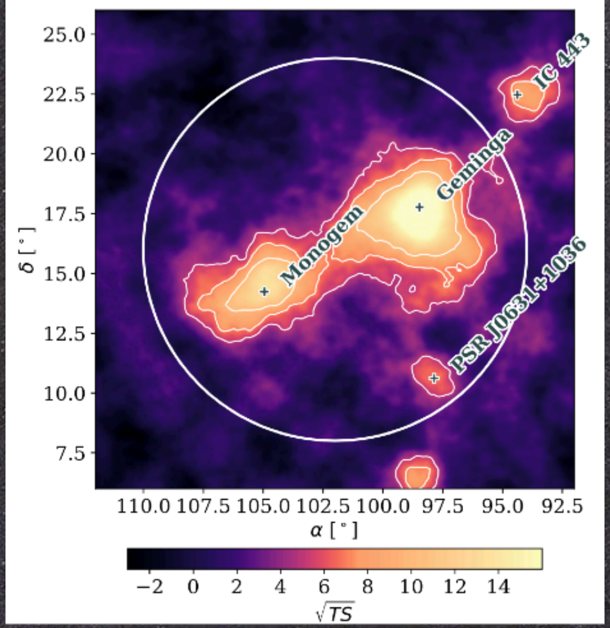

Energy spectrum

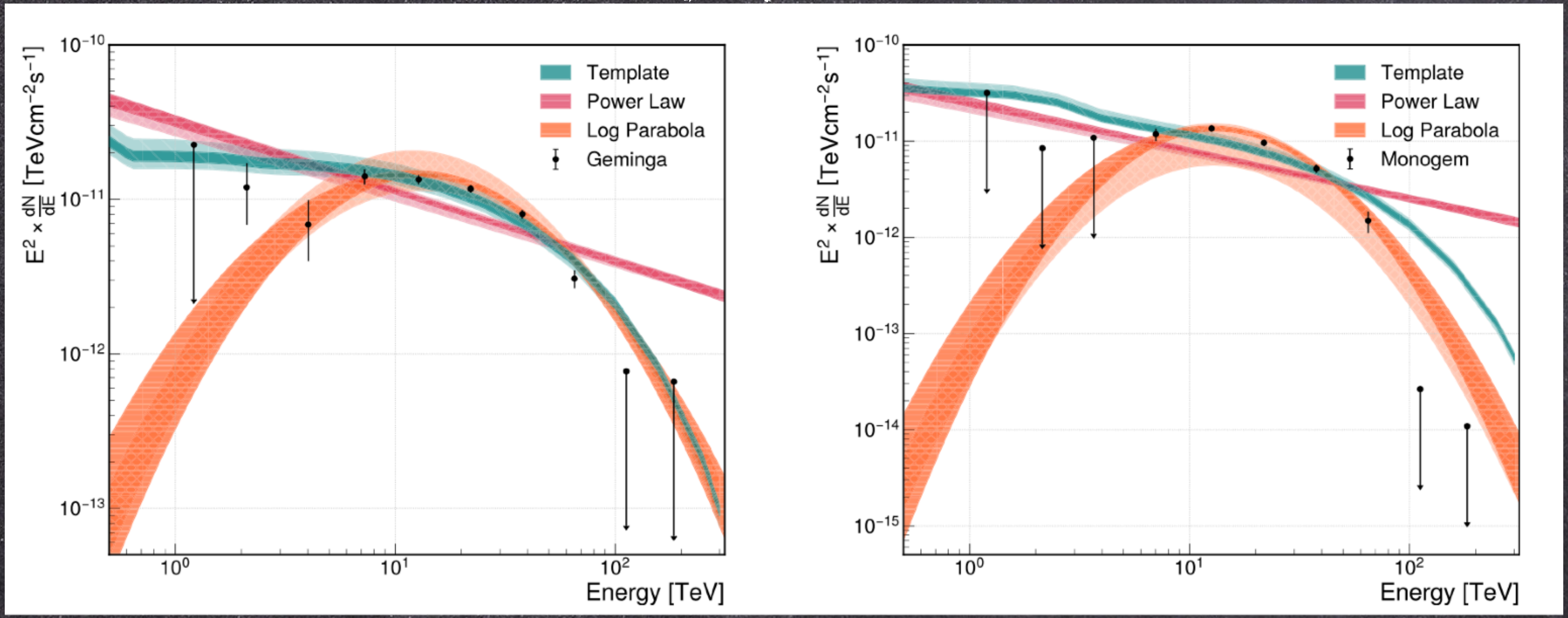

Spectral fit to the data

The template in an ICS physical modelwith suppressed diffusion,

$D(E) \sim 10^{26} (E/1\ \mathrm{GeV})^{\delta}\ \mathrm{cm^2/s}$

HAWC Surface Brghtness for Monogem and Geminga

Albert+ ApJ 2025

Surface brightness in 5.4 - 78 TeV

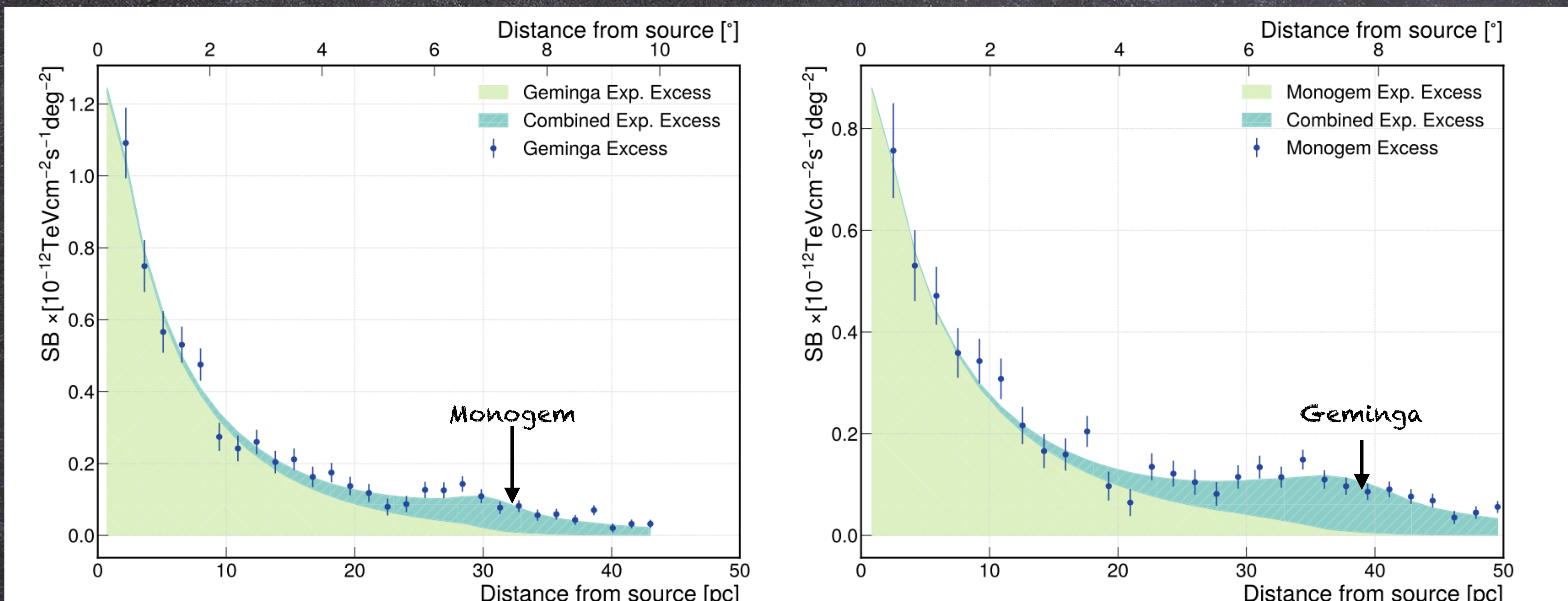

Extension is detected with high precision.

Green area: ICS model with a two-zone diffusion model.

Around the pulsar, the diffusion coefficient is suppressed by ~ 100 wrt the average in the Galaxy.

Does the Geminga γ-ray halo imply slow diffusion around pulsars?

S. Recchia, M. Di Mauro, F. Aharonian, FD, S. Gabici, S. Manconi, PRD 2021

Propagation of electrons is firstly <ins>ballistic</ins> after injection, and becomes diffusive only after multiple deflections on the turbulent circumstellar magnetic field.
The CR transport has three regimes: ballistic ($t \ll t_c$), diffusive ($t > t_c$), and a quasi-ballistic transition.

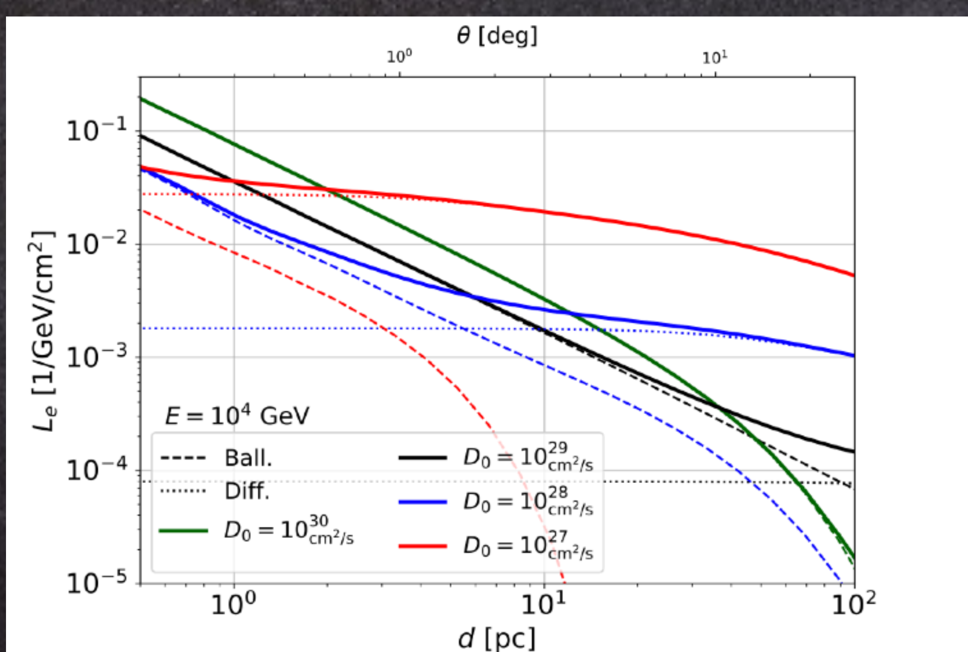

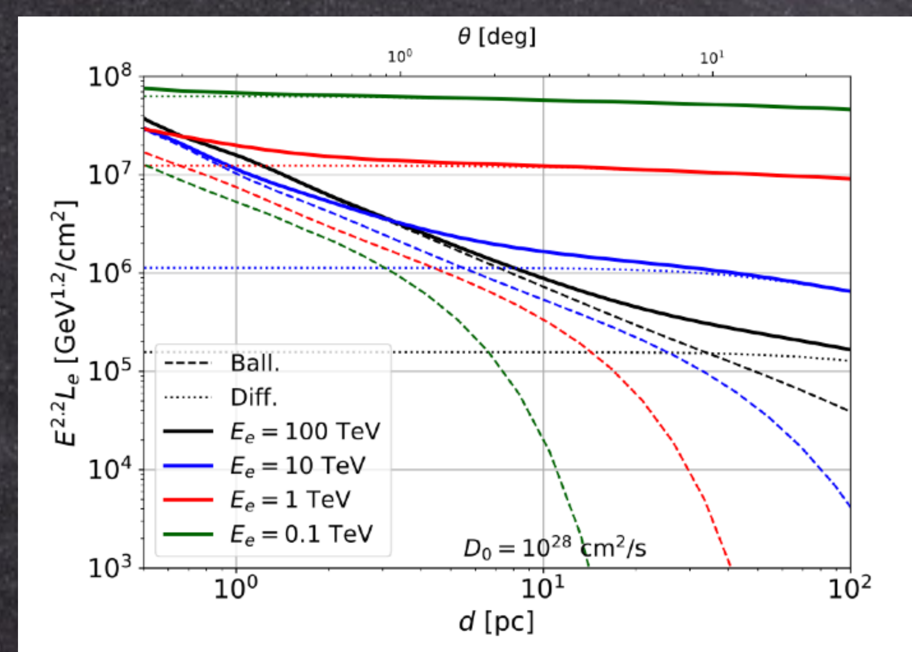

L_e is the e± density integrated along the l.o.s.

This solution offers a simple, physically well motivated interpretation to the observation of the Geminga halo by HAWC

Fitting high energy pulsars surface brightness

S. Recchia, M. Di Mauro, F. Aharonian, FD, S. Gabici, S. Manconi PRD2022

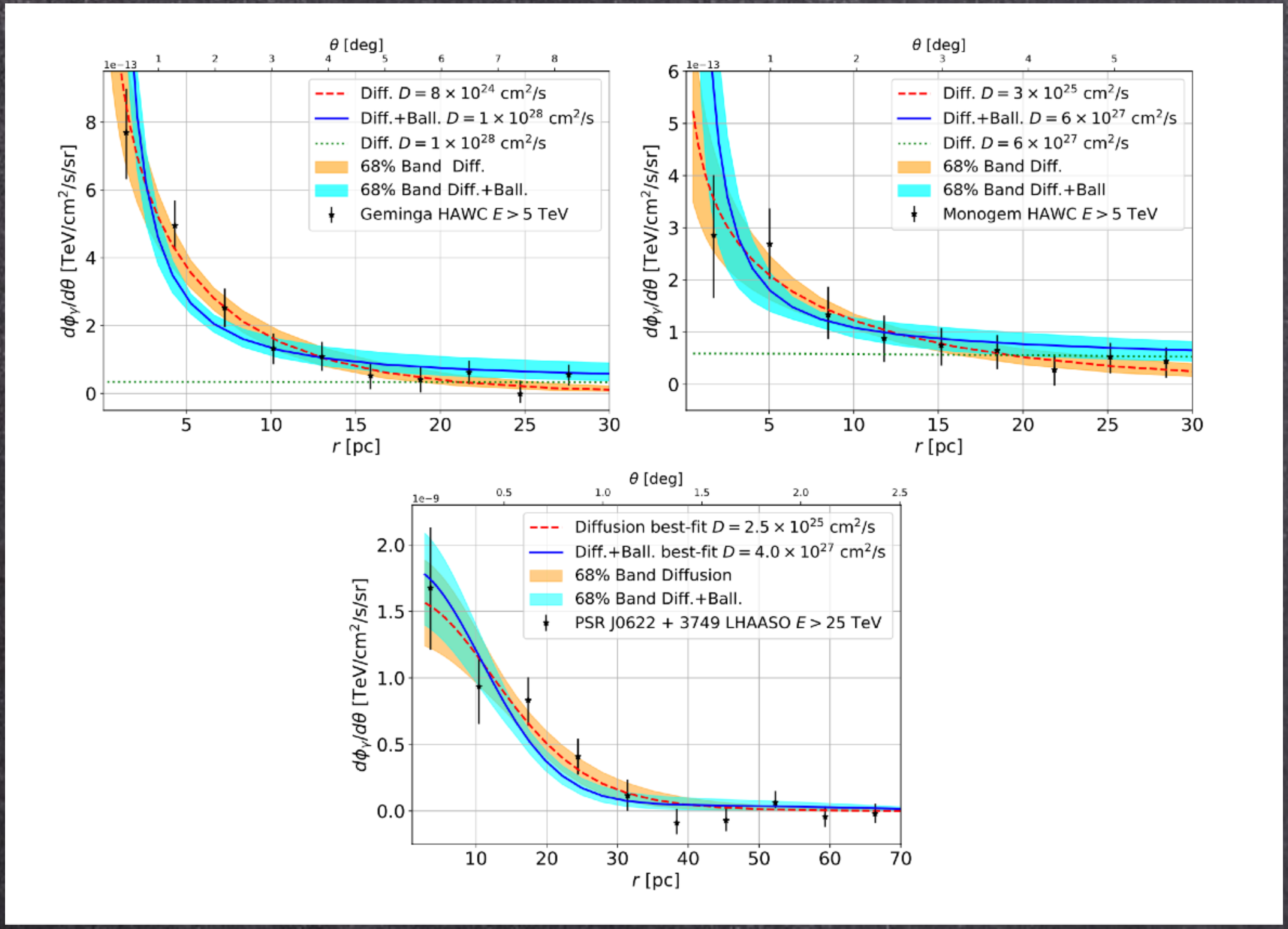

The fit to the surface brightness is very good in all cases both in the diffusive case and in the ballsitic/semi diffuse one.

The efficiency in the ballistic case is high (~ 100%).

Multi-wavelength analysis of sources

Geminga's pulsar halo: an X-ray view

S. Manconi, J. Woo, R. Shang, R.Krivonos, C. Tang, M. Di Mauro, F. D. K. Mori, and C. J. Hailey A&A 2024

A γ-ray halo has been observed in HAWC and Fermi-LAT data.
Interpreted as e± cooling by inverse-Compton scattering.

The same e± emit synchrotron radiation and for a similar X-ray halo

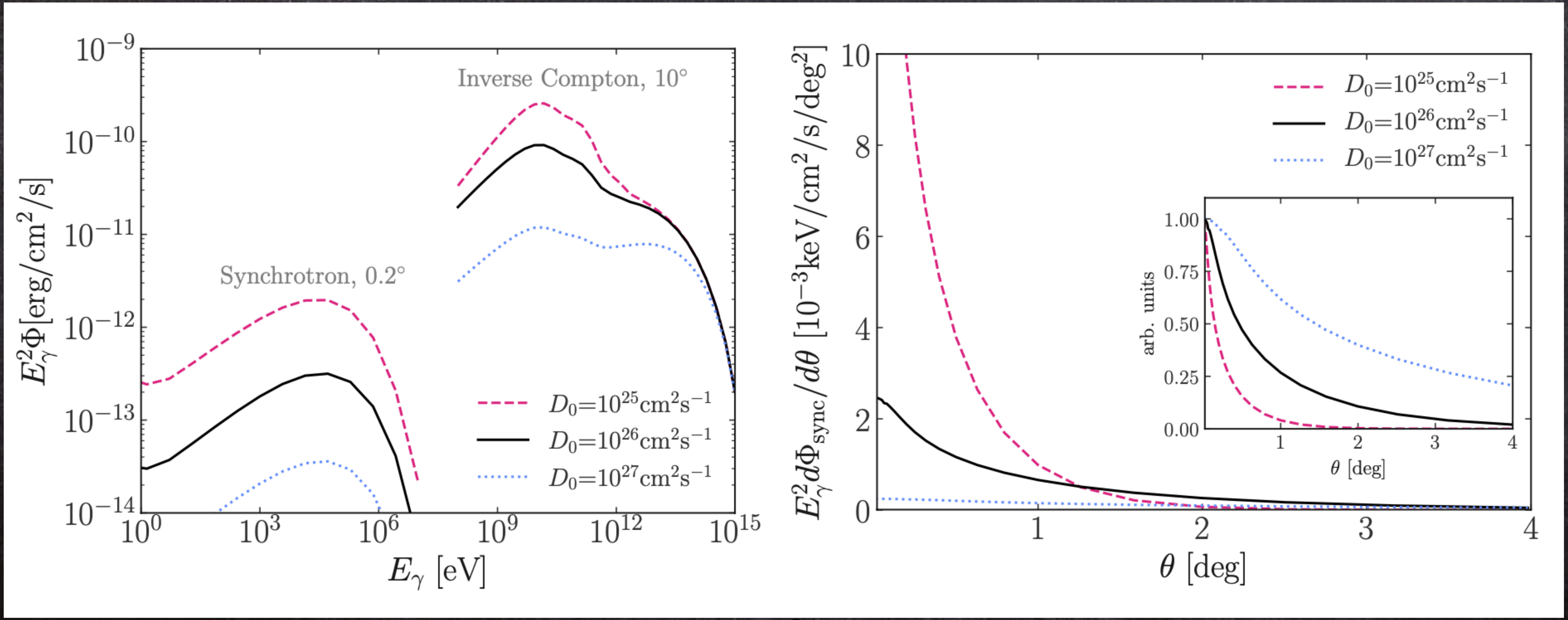

Geminga's pulsar halo: bounds from X-ray data

S. Manconi, J. Woo, R. Shang, R.Krivonos, C. Tang, M. Di Mauro, F. D. K. Mori, and C. J. Hailey A&A 2024

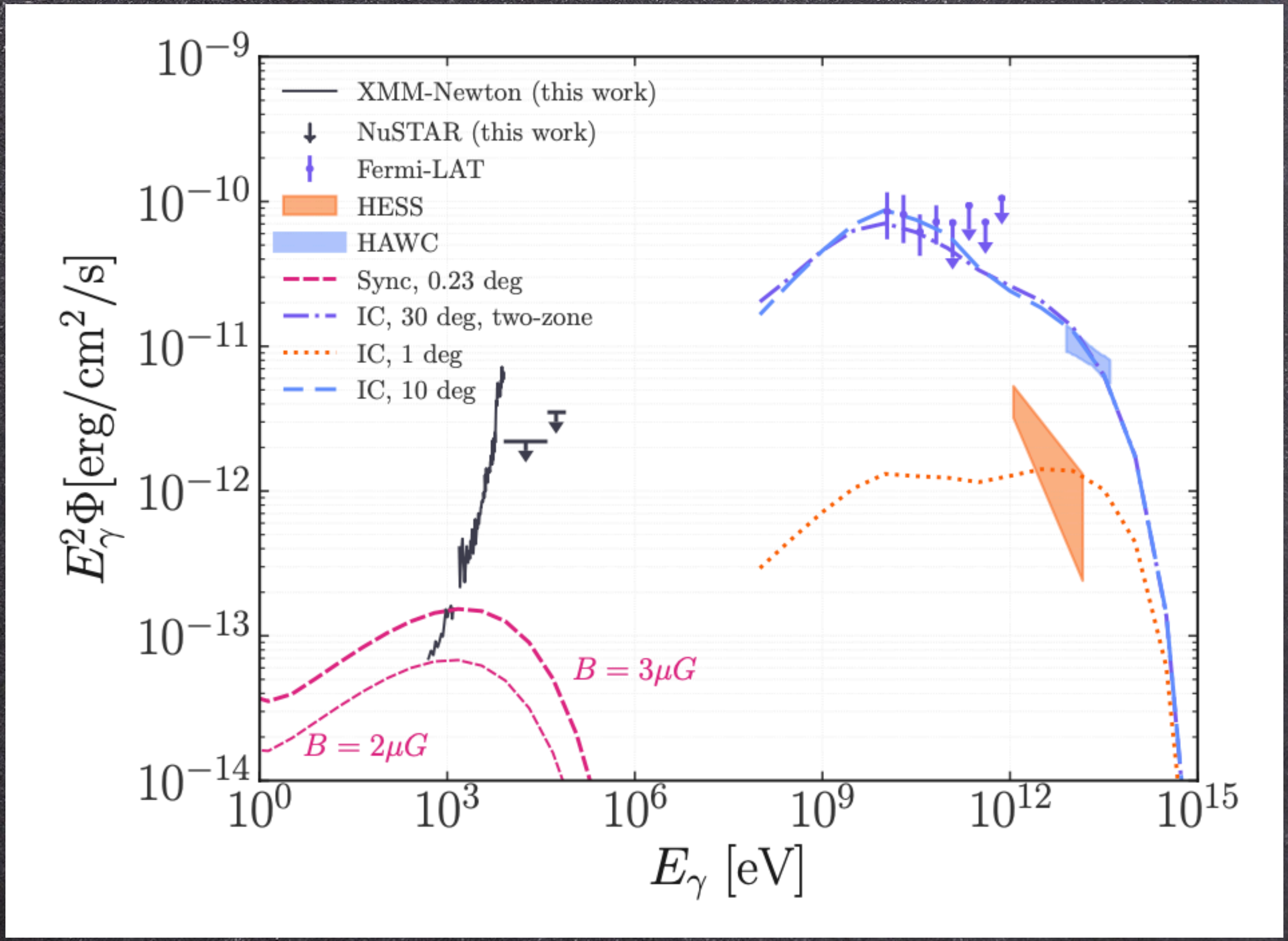

We use archival data in XMM Newton and NUSTAR.
No X-ray halo is detected.
An upper bound on the magnetic field around the pulsar is set to 2 μG

Multi-wavelength observaton of LHAASO J0621+3755 source and first X-ray detection of PSR J0622+3749

Veritas Coll., XMM-Newton Coll., S. Manconi, FD , M. Di Mauro ApJ 2025

Veritas (0.3-10 TeV)

XMM-Newton (0.1-15 keV)

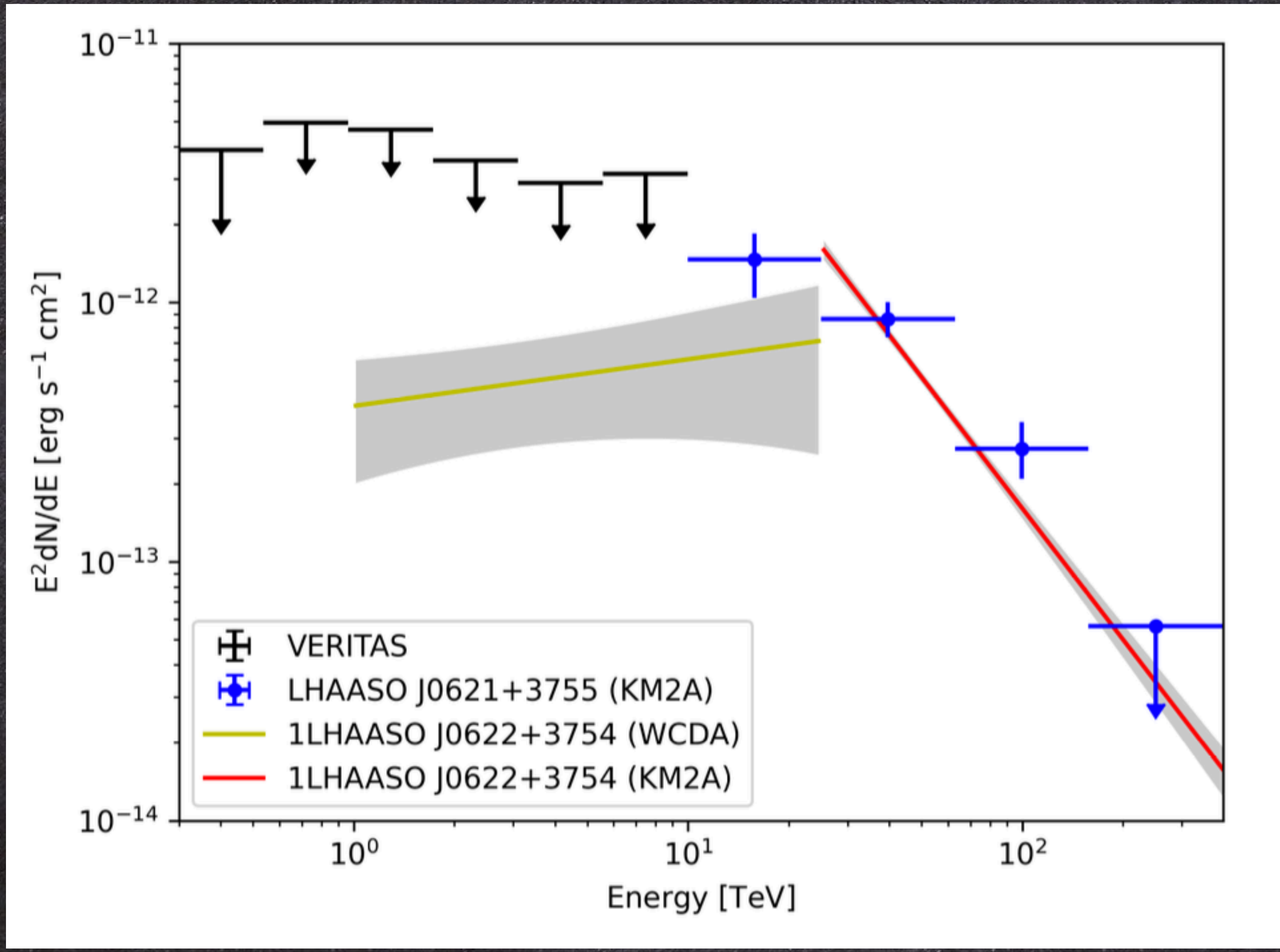

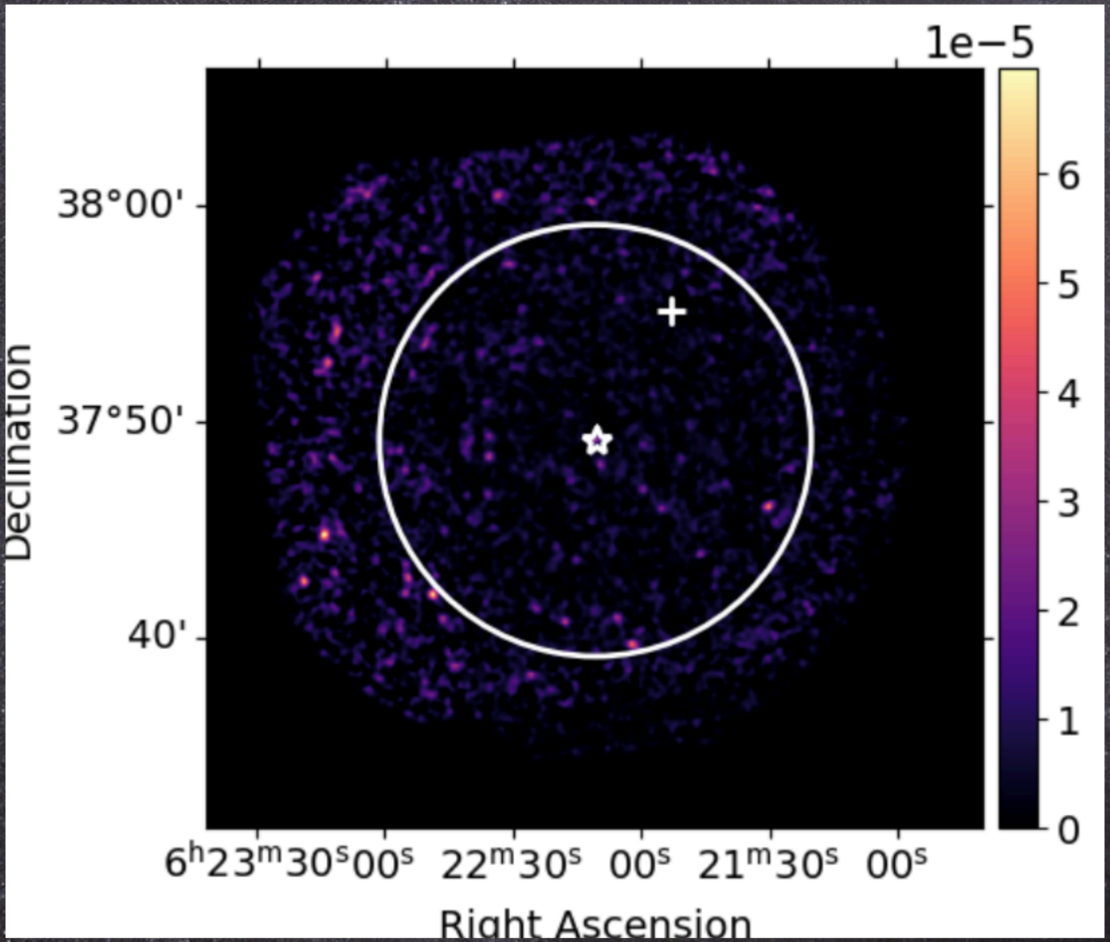

No significant detection in Veritas data

First X-ray detection of PSR J0622+3749

The multi-wavelength SED of LHAASO J0621+3755 as a pulsar HALO

Veritas Coll., XMM-Newton Coll., S. Manconi, FD , M. Di Mauro ApJ 2025

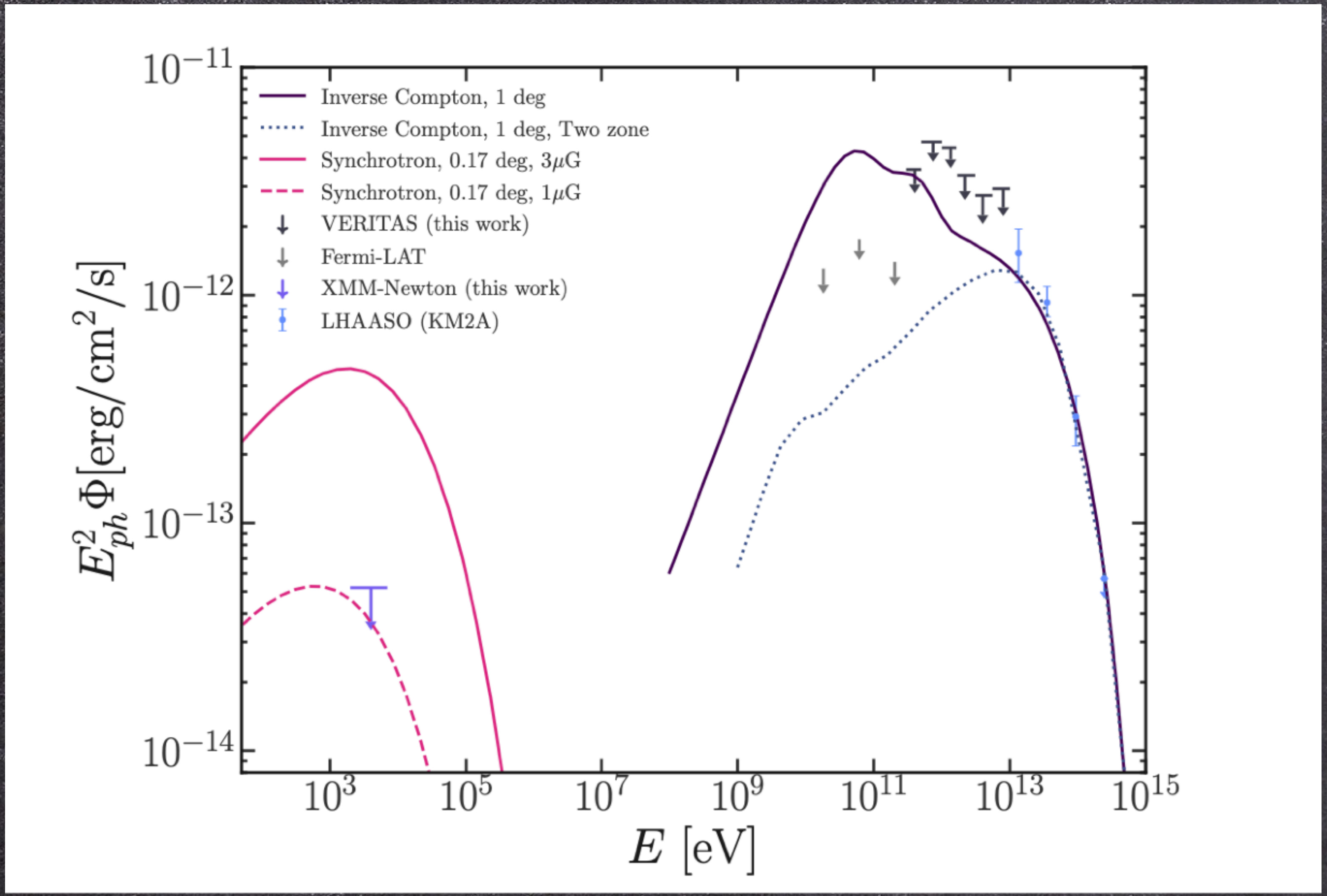

The pulsar halo model is tuned to be compatible with IC emission at TeV energies.

A suppressed diffusion is modeled.

XMM-Newton data constrain the magnetic field B< 1 μG

Conclusions

The $e^{\pm}$ CR flux can be naturally understood in terms of a secondary component, and contributions from SNR (e^-) and PWN (e^+)

CR physics is strongly linked to accelerator data

A small number of catalog pulsars can shape the e^+ flux

γ-ray halo around pulsars open a new window on the complex physics around these sources

Multimessenger analysis are mandatory for a more reliable understanding of pulsar $e^{\pm}$ emission and local diffusion

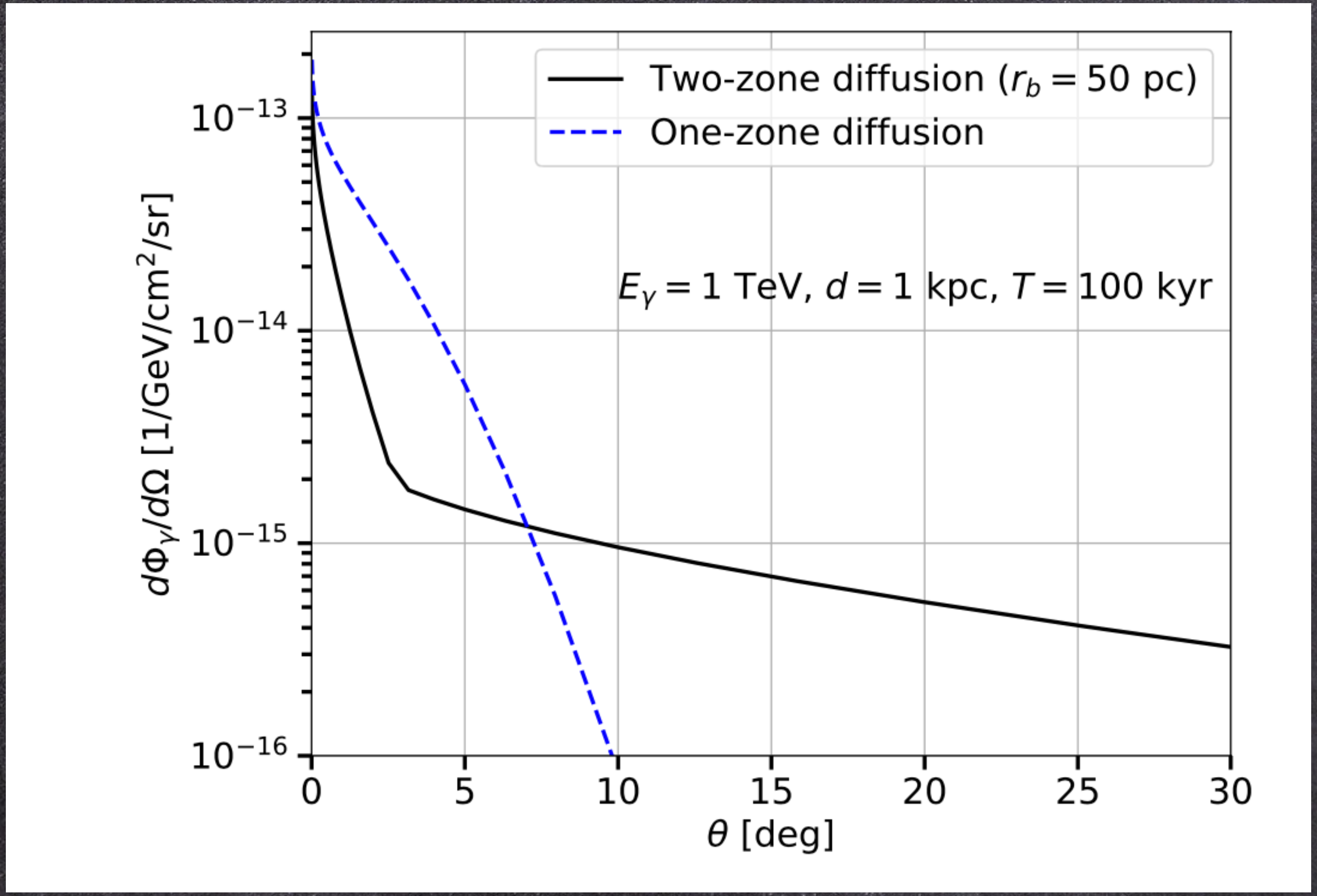

Two-zone diffusion ($r_b = 50$ pc)
One-zone diffusion
$E_\gamma = 1$ TeV, $d = 1$ kpc, $T = 100$ kyr
$d\Phi_\gamma/d\Omega$ [1/GeV/cm^2/sr]
10^{-13}
10^{-14}
10^{-15}
10^{-16}
0
5
10
15
20
25
30
θ [deg]

Brightest pulsars wrt $e^\pm$ emission

τ_0 distribution	τ_0 fixed	Delayed injection	Two zone	Overall	d [kpc]	t [kyr]	$\dot{E}$ [erg/s]
B1055-52	**B1055-52**	**B1055-52**	**B1055-52**	**B1055-52**	0.093	535.0	3×10^{34}
J0633+1746	**J1732-3131**	**J0633+1746**	**J0633+1746**	**J0633+1746**	0.19	342.0	3.2×10^{34}
B0656+14	**J0633+1746**	**B1742-30**	**B1742-30**	**B0656+14**	0.288	111.0	3.8×10^{34}
B0355+54	**J2043+2740**	**B0656+14**	B1738-08	**J1732-3131**	0.64	111.0	1.5×10^{35}
J1732-3131	**B0906-49**	**J2043+2740**	B1749-28	**B0355+54**	1.0	564.0	4.5×10^{34}
J2030+4415	**B0656+14**	B1738-08	J0957-5432	**J2043+2740**	1.48	1200.0	5.6×10^{34}
B0743-53	**B0355+54**	**J1732-3131**	**J2030+4415**	**B1742-30**	0.2	546.0	8.5×10^{33}
J1020-5921	**J0538+2817**	J0954-5430	B0743-53	**J2030+4415**	0.72	555.0	2.2×10^{34}
J0954-5430	**J2030+4415**	**J2030+4415**	J0945-4833	**B0906-49**	1.0	112.0	4.9×10^{35}
B1742-30	J1016-5819	**B0355+54**	B1001-47	**J0538+2817**	1.3	618.0	4.9×10^{34}

Model for ICS around LHAASO J0621+3755

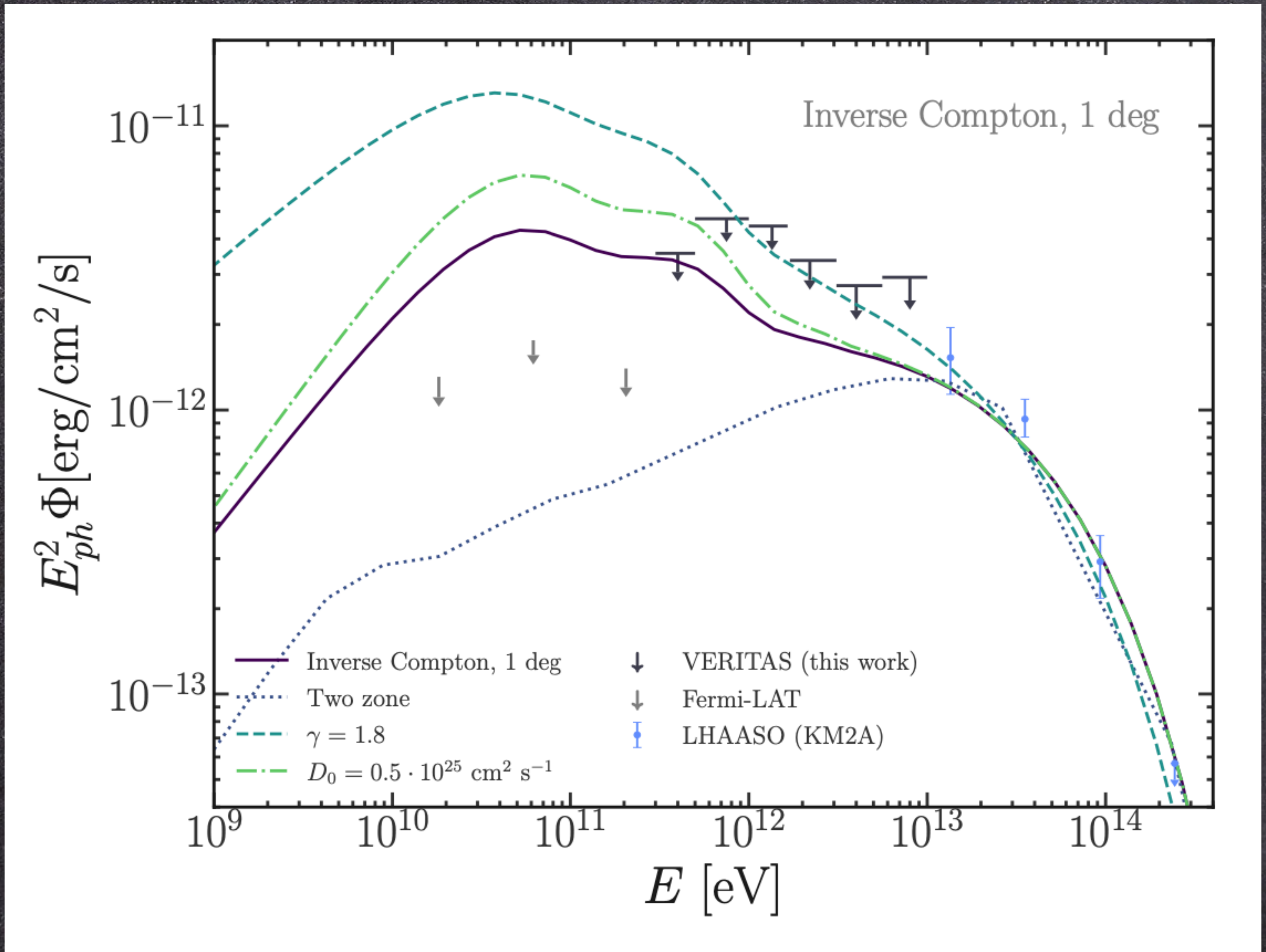

Benchmark model: $D=2\times10^{25}$ cm²/s, $e^{\pm}$ injection index 2.4, efficiency 0.20